LIGHT SCATTERING PROPERTIES VARY ACROSS DIFFERENT REGIONS OF THE ADULT MOUSE BRAIN

by

SAIF I. AL-JUBOORI

B.S., Nahrain University, 2008

A thesis submitted to the

Faculty of the Graduate School of the

University of Colorado in partial fulfillment

of the requirements for the degree of

Master of Science

Electrical Engineering

2013

This thesis for the Master of Science degree by

Saif I. Al-Juboori

has been approved for the

Electrical Engineering Program

by

Tim Lei, Chair

Achim Klug

Yiming Deng

July 8, 2013

Al-Juboori, Saif, I. (M.S., Electrical Engineering)

Light Scattering Properties Vary across Different Regions of the Adult Mouse Brain

Thesis directed by Assistant Professor Tim Lei.

ABSTRACT

Recently developed optogenetic tools provide powerful approaches to optically excite or inhibit neural activity. In a typical in-vivo experiment, light is delivered to deep nuclei via an implanted optical fiber. Light intensity attenuates with increasing distance from the fiber tip, determining the volume of tissue in which optogenetic proteins can successfully be activated. However, whether and how this volume of effective light intensity varies as a function of brain region or wavelength has not been systematically studied.

The goal of this study was to measure and compare how light scatters in different areas of the mouse brain. We delivered different wavelengths of light via optical fibers to acute slices of mouse brainstem, midbrain and forebrain tissue. We measured light intensity as a function of distance from the fiber tip, and used the data to model the spread of light in specific regions of the mouse brain. We found substantial differences in effective attenuation coefficients among different brain areas, which lead to substantial differences in light intensity demands for optogenetic experiments. The use of light of different wavelengths additionally changes how light illuminates a given brain area. We created a brain atlas of effective attenuation coefficients of the adult mouse brain, and integrated our data into an application that can be used to estimate light scattering as well as required light intensity for optogenetic manipulation within a given volume of tissue.

The form and content of this abstract are approved. I recommend its publication.

Approved: Dr. Tim Lei

DEDICATION

I dedicate this work to those beloved ones whom I have lost and I still remember; to those who are suffering, not only every single day, but every single moment hoping that there will be a day in which researchers, like us, will come up with treatment for their illnesses to mitigate their suffering and alleviate their pain; to those whom I have promised that I am going to do my best in participating in whatever is going to be available for me to pave the way for breakthroughs that will lead to a better life with less pain and more pleasure for them and their dearest ones; to those whom I gave my words to that I will never let them down; to people whom I am always looking forward to putting a smile on their faces.

ACKNOWLEDGMENTS

I acknowledge my fellowship from the Higher Committee for Education Development in Iraq (HCED).

I would like to thank my consultant, advisor, and mentor, Dr. Tim Lei for all his encouragement, support, consultation, and advising that he has bestowed upon me throughout my graduate studies. Without his help, I would not have been able to spend my time, day by day, in a scientific and intellectual milieu which has been giving me the chance to learn from, study, meet, and collaborate with incredible researchers and students who have had a great influence on me. I am honored to work under his supervision.

Here, I would also like to thank Dr. Achim Klug, Dr. Gidon Felsen, Dr. Anna Dondzillo, and Dr. Elizabeth Stubblefield for their collaboration in this work. I am indeed grateful for having this wonderful opportunity collaborating with all of them. It has been such an enriching experience being around people of knowledge like them.

TABLE OF CONTENTS

CHAPTER

LIST OF TABLES

Table

LIST OF FIGURES

Figure

CHAPTER I

INTRODUCTION

Optogenetics Era

Deep brain stimulation (DBS) technology is one of the most effective technologies that have been used as a treatment and a cure for a wide spectrum of psychiatric disorders and diseases. The key function of this technology is making various kinds of stimulation to specific defective areas that are responsible for certain brain's functions by either activate or deactivate them to compensate for the malfunction that is happening in them. The conventional approach to this technology is by doing the stimuli electrically by inserting metal electrodes in those areas and implementing that required current intensity to achieve the pre-decided aim. However, as one can see, there are some downsides to this method though. Cells damage, corrosions, tumors…etc., are predisposed by this invasive method [1]. It might also have a severe effect on the surrounding and the intact cells. In addition, metal electrodes can not specifically target a certain cell type in the neural target, making the treatment much less specific and could lead to adverse treatment outcomes. Moreover, it is not possible to specifically control stimulation or suppression of the neural signals in the brain. Nonetheless, DBS using metal electrodes is the current state-of-the-art method of deep brain stimulation. After discovering some photosensitive materials especially photosensitive proteins that could be latched on cells and cells' membranes, the idea of using light to do the same required stimuli, but this time optically, came out to the surface as a safer and noninvasive breakthrough to deal with these conditions and diseases [2]. In this method, the light is

shining specific areas which have already those photosensitive proteins, and some parts of the neural networks start to fire or suppress that firing and control some brain functions to deliver the desired treatment. This is what is called “optogenetic” technique, in brief! [2] And nowadays, it is considered as one of the recent cutting edge technologies in this field. And from this point forward, manipulating neural function with light is becoming an increasingly important technique. This is particularly important for this recently emerging field of optogenetics, which provides powerful tools to either activate or suppress neural activity with light at a relatively fast time scale (sub-millisecond) (e.g. [3]-[5]). Controlling neuronal firing with light has opened up not only a number of exciting new avenues to study neural circuits, but also treatment options of a number of medical conditions such as Parkinson’s disease or certain forms of blindness [6]-[8].

As it has been known for the conventional approach that the amount of charge intensity will specify the demanded treatment as the brain areas have different electrical properties, the amount of light (or the light intensity) required to serve the same purpose should be pre-specified as well, as those brain areas may show different optical properties. Having said that, the first question that have been asked is; how much optical power intensity that is required to deliver light to a specific neural target with a specific optical penetration depth to get the stimulation, activation or deactivation, and the neural responses desired will be. After determining this amount of the power intensity required to do the process, the second question is, what is the initial optical power intensity that the physician should start with at the outer boundary of the neural target- as it is not preferable to punch through it, yet instead, shining light directly on top of it.

The latter question requires the knowledge of the optical properties for those areas under study or investigation, because it is related to the light transmission, absorption, and the scattering phenomena that are happening within the targeted area. Therefore, the idea of having a three-dimensional (3D) light scattering model has become a necessity in order to give a comprehensive expectation of how light behaves inside different brain areas. Yet, it has been required to collect the constructing optical parameters of this light scattering model. Thus, the scientific journey has started by conducting this study to achieve this goal by extracting the effective attenuation coefficient (μ_t) which is one of the main optical parameters that this model will be composed of.

Neuroscience-Optogenetics Experimental Insights

For experiments using cell cultures or brain slices, the precise and reliable delivery of light to the neurons to be manipulated is relatively simple and is typically achieved by attaching a suitable light source to a microscope, and subsequently delivering light stimuli with the desired parameters directly to the neural tissue. For *in-vivo* experiments, however, light delivery to deep brain areas is much more challenging. Typically, investigators use stereotaxic methods to place an optical fiber just above the brain neural target to be illuminated, such that light emitting from the fiber effectively illuminates the tissue below the fiber tip [9].

Depending on the optical properties of the specific tissue, light emitted from the fiber tip propagates deeper or less deep through the tissue, with neurons more distant from the fiber tip receiving higher or lower light intensities. All light sensitive molecules (such as the various opsins typically used in optogenetic experiments, but also caged compounds and fluorescent dyes) have a threshold of activation, (for the purpose of this

publication defined in practical terms as the minimum light intensity required to effectively trigger or inhibit the desired neural action potential). Therefore, light sensitive molecules can only be activated at a certain maximum distance from the light source, and this distance depends on both the optical properties of the tissue and the activation threshold of the molecule used in the experiment. Most studies involving delivery of light to deep brain areas assume, for simplicity, that all brain tissue scatters light in the same way, i.e. different brain areas behave similarly if not identically as far as light propagation in the tissue is concerned [1], [10], [11]. However, some brain areas consist primarily of cell bodies while others consist primarily of neural fibers, and some brain areas with significant myelination appear darker while others appear lighter when observed under a microscope with transmitted light, suggesting differences in optical properties between different brain areas.

Main Goals of This Study

The primary goal of this study was to test the hypothesis that different brain areas scatter and propagate light to different degrees. If correct, specific knowledge about the brain area to be manipulated would be required for the appropriate design of experimental manipulations. A secondary goal of the study was to create an easy to use computer program to estimate light scattering values for different areas of the mouse brain that could be used as a reference in future experiments.

Our experimental approach was to use sections of fresh brain tissue in combination with light emitting optical fibers that were advanced through the tissue to precisely measure light scattering properties. The results presented here are supplemented with a light scattering mouse brain atlas programmed as an iPhone application. These

tools are intended to aid an investigator in determining the required light intensity to be delivered for successful optogenetic manipulation.

Ethics Statement

All animal procedures were approved by the Institutional Animal Care and Use Committee (IACUC) of the University of Colorado Medical Campus (Permit number B-88412(05)1D. Furthermore, all applicable laws and regulations, as well the PHS Policy were strictly followed.

Animal Subjects

34 male and female C57BL/6J mice were used in these experiments. All animal procedures were approved by the University of Colorado Institutional Animal Care and Use Committee, and were conducted in accordance with National Institutes of Health standards on humane treatment of laboratory animals.

Thesis Orientation

In the following chapters, the experimental setup, sample preparation, targeted brain areas, and experimental procedure needed to measure effective attenuation coefficients will be presented (Chapter II). The results of these sets of experiments and the brain atlas establishment will be shown, as well, in both graphical and numerical presentations in Chapter III. These results will also be discussed, summarizing the main findings of this study, in Chapter IV, and some impairment will be illustrated in one of these sections. Finally, solutions for those difficulties that have worked out so far, improvements that have been come up with, some other suggestions, comparison with previous studies, and future plans (research proposal for gathering more parameters to

perfect a three-dimensional (3D) light scattering model of the mouse brain) will also be available to the researcher in Chapter V.

CHAPTER II

EXPERIMENTAL SETUP, SAMPLE PREPARATION, TARGETED BRAIN AREAS, EXPERIMENTAL PROCEDURE, AND LIGHT PROFILE AND TISSUE DAMAGE CONTROL EXPERIMENTS

Experimental Setup

The experimental setup is mainly composed of the following devices: an inverted microscope (Nikon Diaphot 200, Nikon Corp., Japan) with a monochromatic 12bit Charged-Coupled Device (CCD) camera (Mightex CCE-B013-U) attached to it, a current derive source- a Mightex LED power supply (SLB-1200-1)- which derives the optical fibers, a computer, a CCD video camera and a monitor. The latter two components have been added afterward to adjust the fiber tip precisely on top of the sample before starting running the experiment. The investigational bench is pictured in figure II.1.

Figure II.1 The experiment's desk showing the experimental setup equipment

Optical Fiber Assembly

Three different optical fiber assemblies were used for the measurements. All three assemblies consisted of 100 µm core diameter optical fibers (UM22-100, Thorlabs, Newton, NJ)) attached to 453 nm (blue), 528 nm (green), and 940 nm (near infra-red) LEDs, respectively. All LEDs were purchased from Digikey (Thief River Falls, MN). The optical fiber was lined up with its respective LED using two precision manipulators. The alignment was carefully done to obtain maximum optical throughput but avoiding crashing the fiber tip into the LED. UV optical epoxy was used to set the optical fiber in place and to secure the alignment between the LED and the optical fiber. In each case, the LED-optical fiber assemblies were powered by the Mightex LED power supply, allowing the optical power output to be adjusted by changing the electrical current running through the LEDs. Each and every experiment, the fiber optics should be examined not only to make sure that the output optical power intensity is steady but also the fiber tips are still intact and having a uniform light profile. Figure II.2 shows the optical fiber output light profile, whereas figure II.3 and figure II.4 illustrate how this light profile would be after traveling through 100 µm and 200 µm tissue thickness for the same exposure time (2500 ms). Another example when the exposure time has changed for the same tissue thickness is presented in figure II.5 and figure II.6.

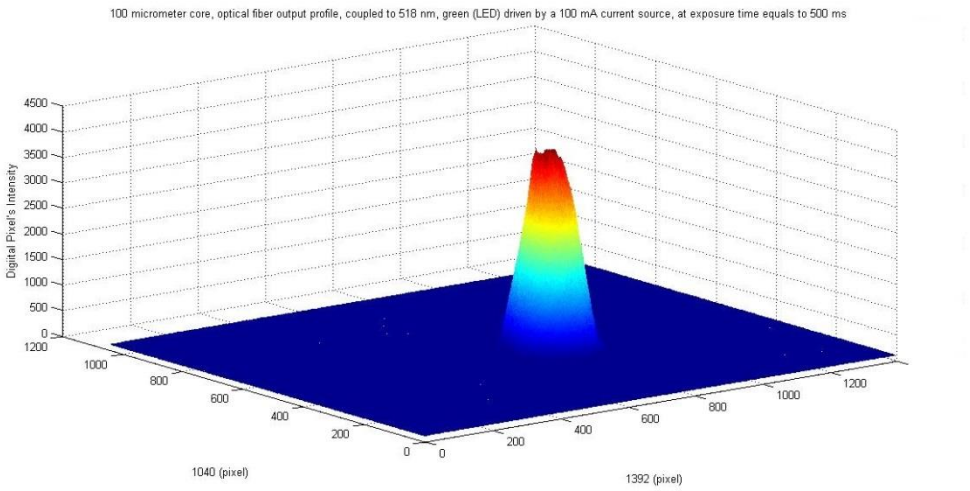

Figure II.2 A 100 μm core, coupled to a 518 nm green LED and driven by a 100 mA current source, optical fiber output profile

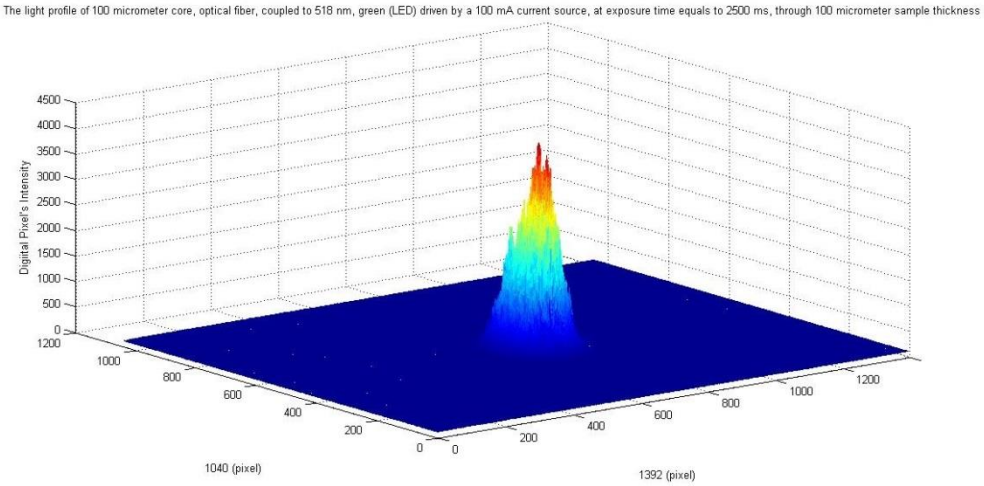

Figure II.3 A 100 μm core, coupled to a 518 nm green LED and driven by a 100 mA current source, optical fiber output profile after traversing a 100 μm sample thickness

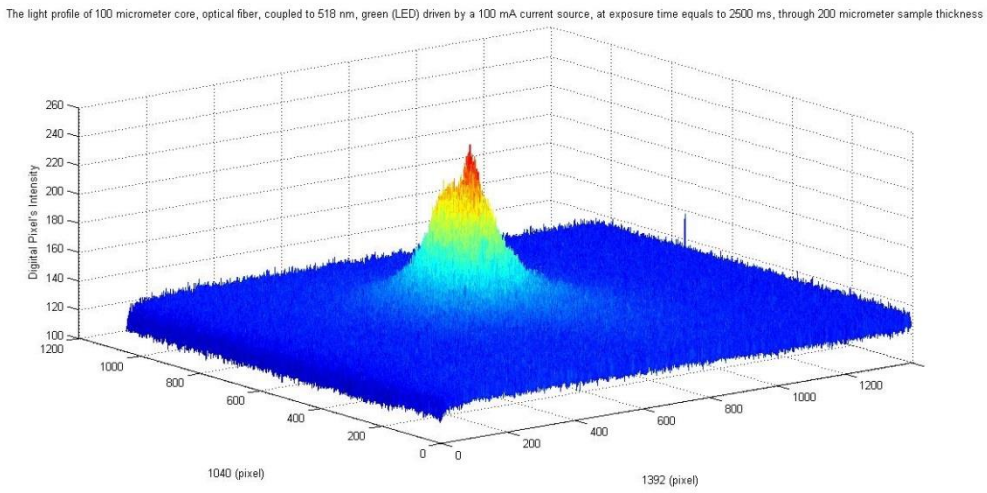

Figure II.4 A 100 μm core, coupled to a 518 nm green LED and driven by a 100 mA current source, optical fiber output profile after traversing a 200 μm sample thickness

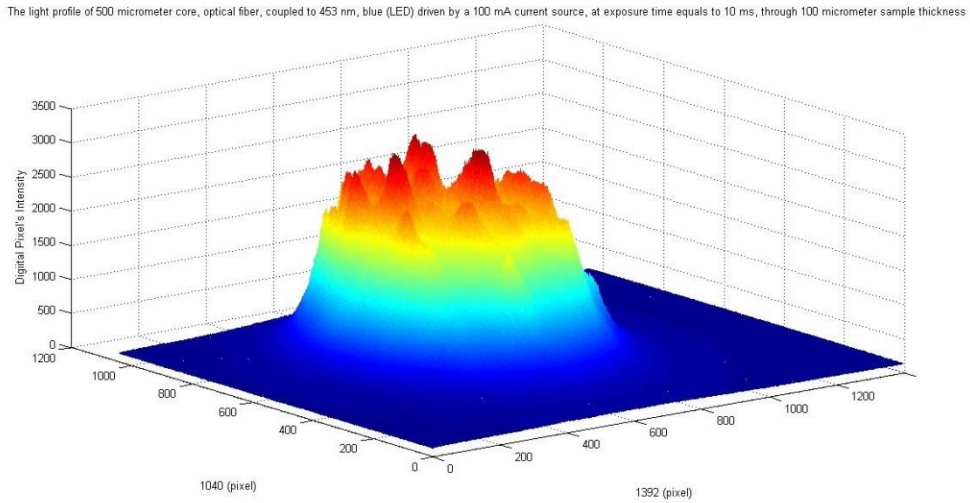

Figure II.5 A 500 μm core, coupled to a 453 nm blue LED and driven by a 100 mA current source, optical fiber output profile after traversing a 100 μm sample thickness at 10 ms exposure time

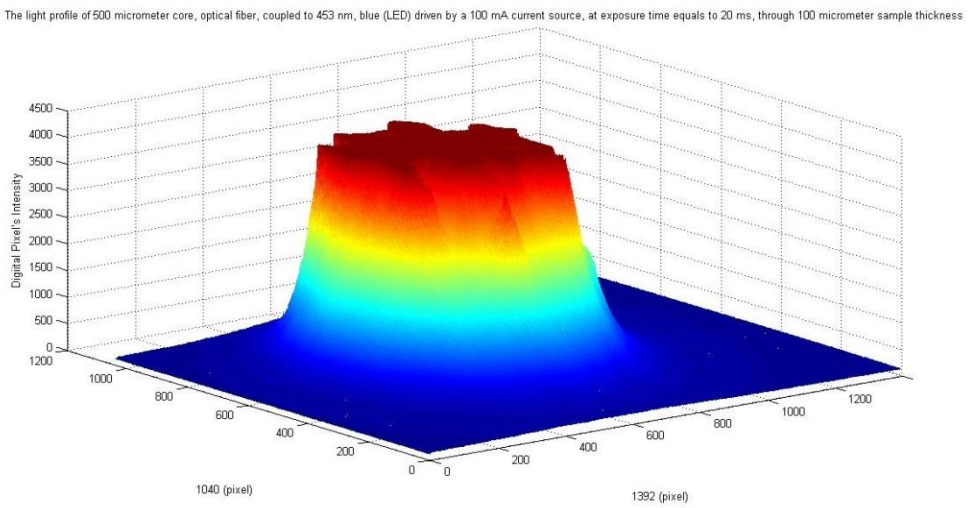

Figure II.6 A 500 μm core, coupled to a 453 nm blue LED and driven by a 100 mA current source, optical fiber output profile after traversing a 100 μm sample thickness at 20 ms exposure time

Linearity Tests

The Importance of These Linearity Tests

Now that these first sets of graphs had been collected and made as empirical references for the next following sets of experiments that have been launched after. And that has given the flexibility required to modify and adjust some experimental parameters without changing the setup or the procedure entirely. In addition to that, comparable ways of presenting the analyzed data and the results have been allowed by the aid of those graphs.

LEDs Power Intensity Linearity Tests

Four different types of optical fibers coupled to four different LEDs having different wavelengths had been tested to incorporate within this experiment; those fibers

are: green 518 (nm), 100 (µm) core diameter, green 528 (nm), 100 (µm) core diameter, blue 453 (nm), 100 (µm) core diameter, blue 453 (nm), 500 (µm) core diameter. The power intensity graph as a function of current intensity had been measured for those four optical fibers and drawn as they can be seen in the following figures. The CCD camera sensitivity for LEDs power intensity linearity responses under normal room's illumination versus when the room light is turned off had been tested taking into account the different LEDs wavelengths and different optical fibers core diameters. The results show very reliable linearity responses for the camera.

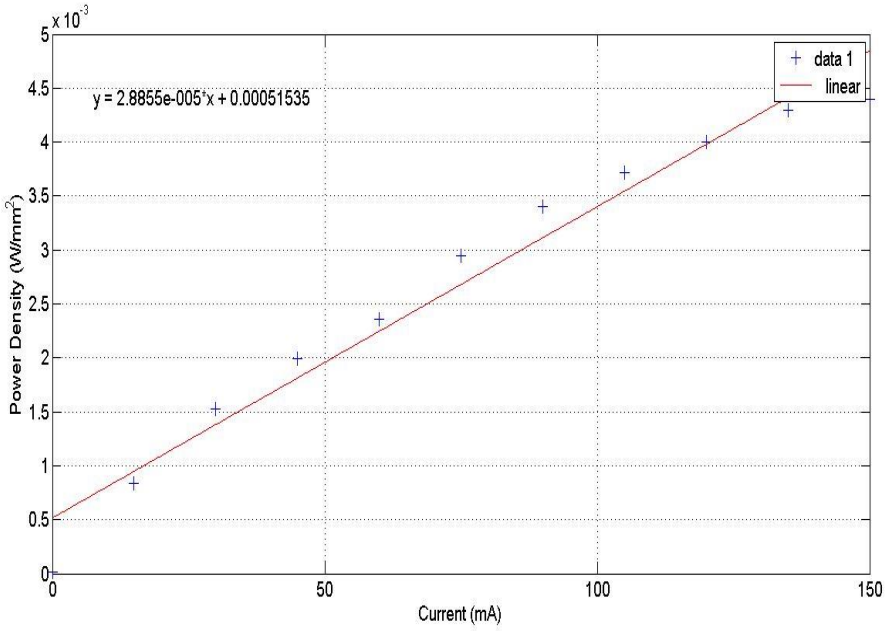

Figure II.7 The data fitting line for the output power density of the 100 µm core optical fiber, coupled to a 518 nm green (LED), when the room light is turned off

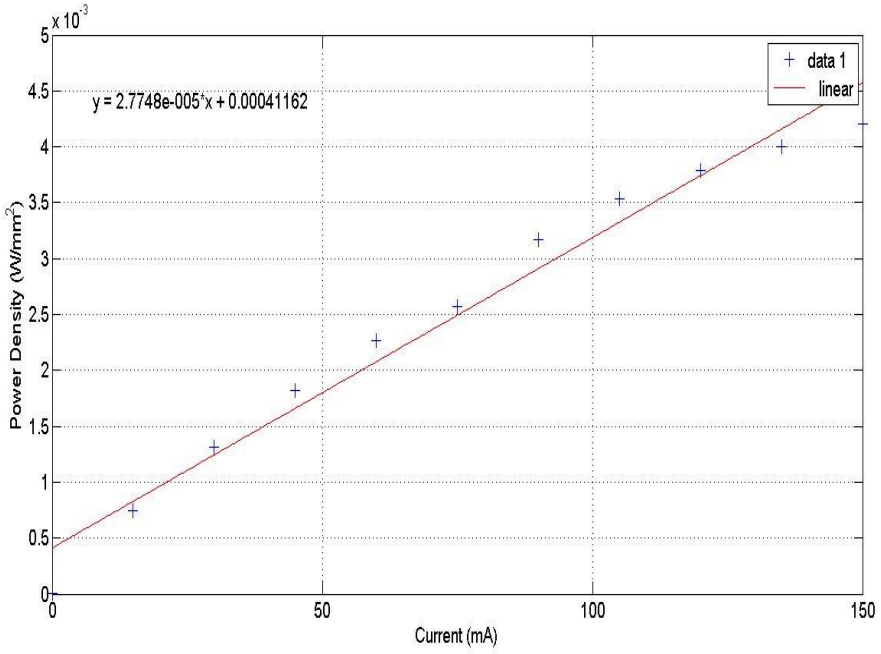

Figure II.8 The data fitting line for the output power density of the 100 µm core optical fiber, coupled to a 518 nm green (LED), under normal room's illumination

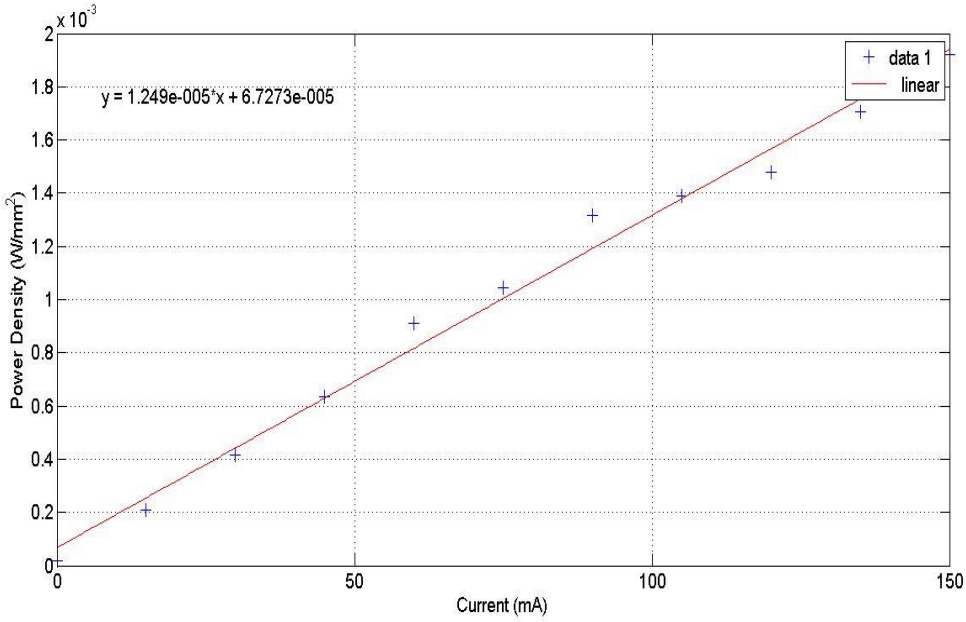

Figure II.9 The data fitting line for the output power density of the 100 µm core optical fiber, coupled to a 528 nm green (LED), when the room light is turned off

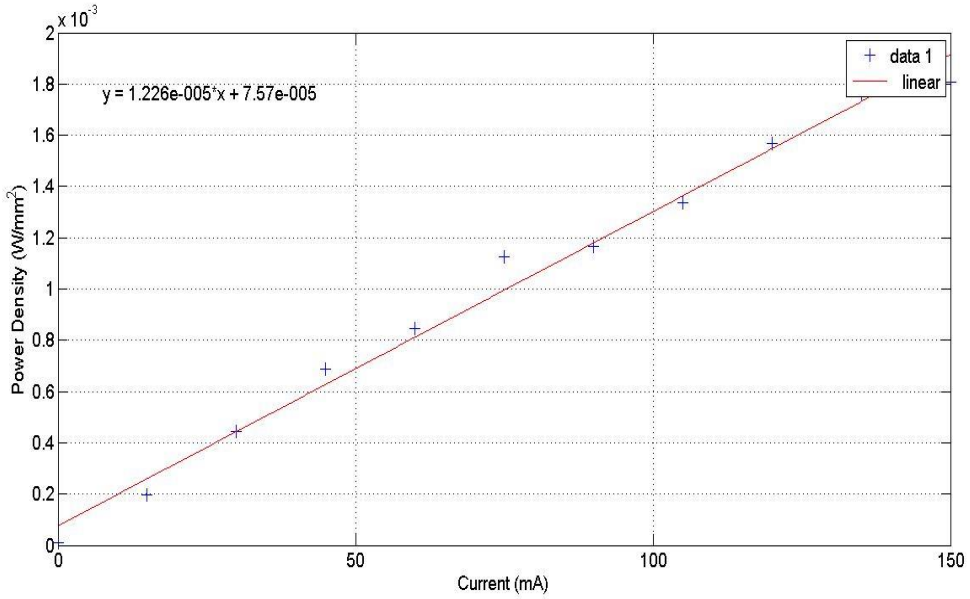

Figure II.10 The data fitting line for the output power density of the 100 µm core optical fiber, coupled to a 528 nm green (LED), under normal room's illumination

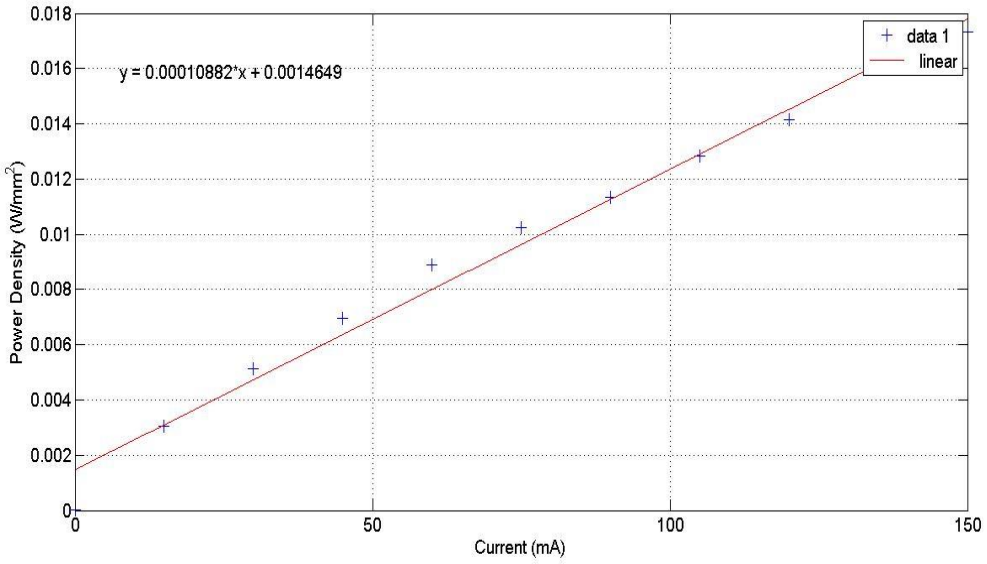

Figure II.11 The data fitting line for the output power density of the 100 µm core optical fiber, coupled to a 453 nm blue (LED), when the room light is turned off

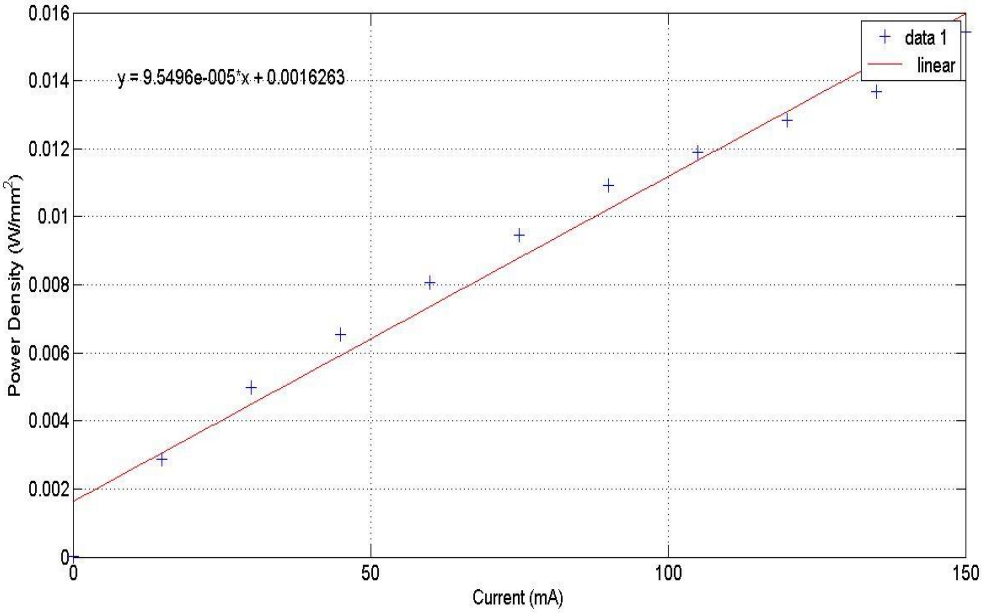

Figure II.12 The data fitting line for the output power density of the 100 µm core optical fiber, coupled to a 453 nm blue (LED), under normal room's illumination

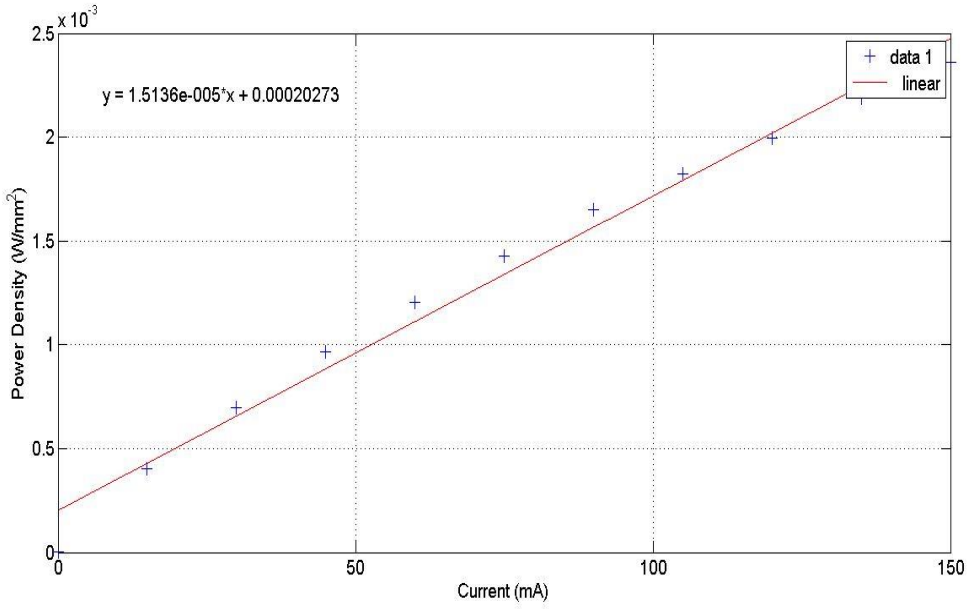

Figure II.13 The data fitting line for the output power density of the 500 µm core optical fiber, coupled to a 453 nm blue (LED), when the room light is turned off

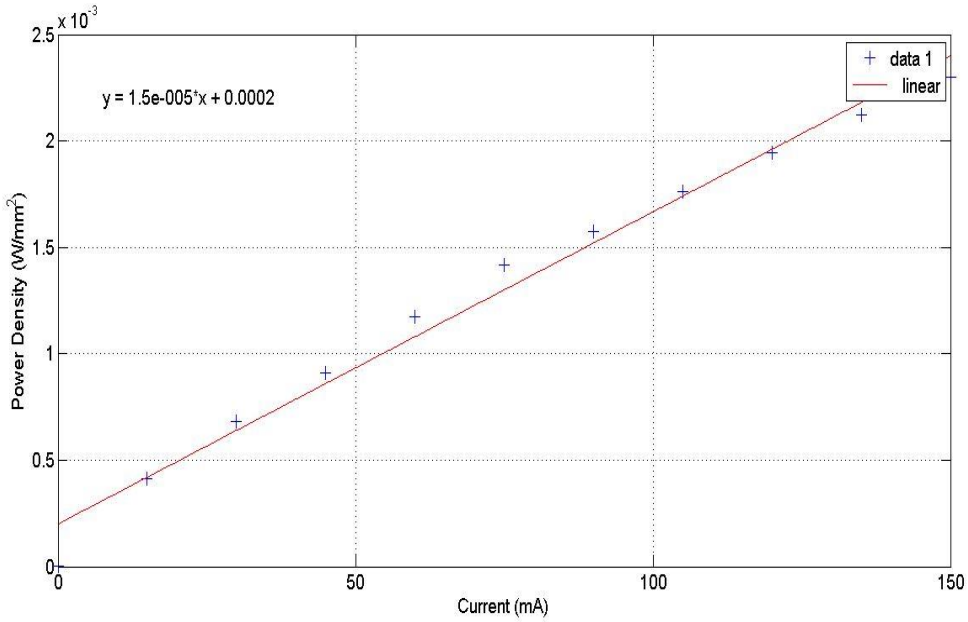

Figure II.14 The data fitting line for the output power density of the 500 µm core optical fiber, coupled to a 453 nm blue (LED), under normal room's illumination

CCD Camera Linearity Tests

The CCD camera linearly tests had also been experimented as a function of various exposure times and these graphs can be shown in the following figures. Five different pixel locations had been taken into consideration which are (100, 100), (100, 1292), (520, 696), (940, 100), and (940, 1292) of (1040 x 1392) pixels image to show the consistency and robustness of the linearity responses across the entire detection area.

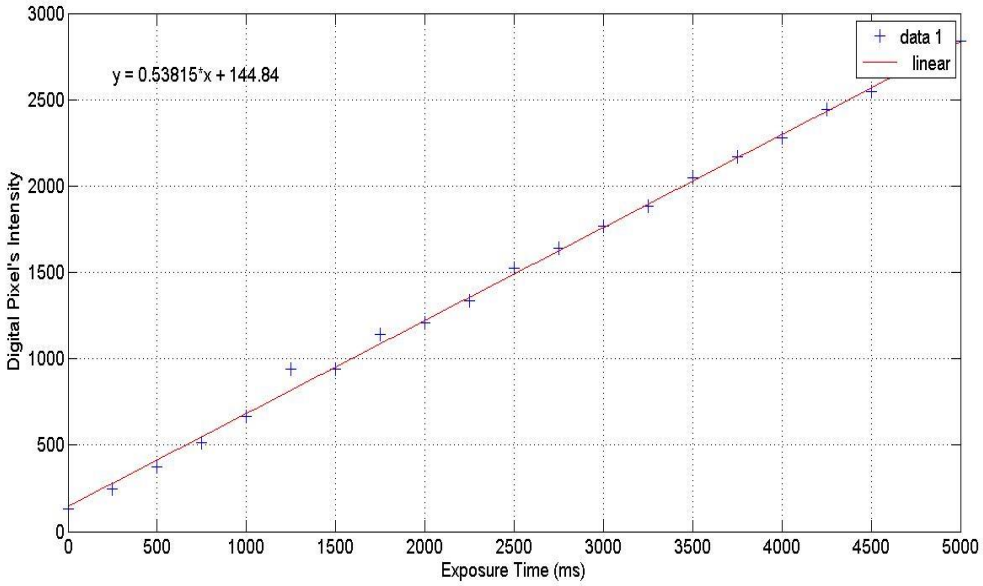

Figure II.15 Linearity test for the CCD camera at (100, 100) pixel's location of (1040 x 1392) pixel image

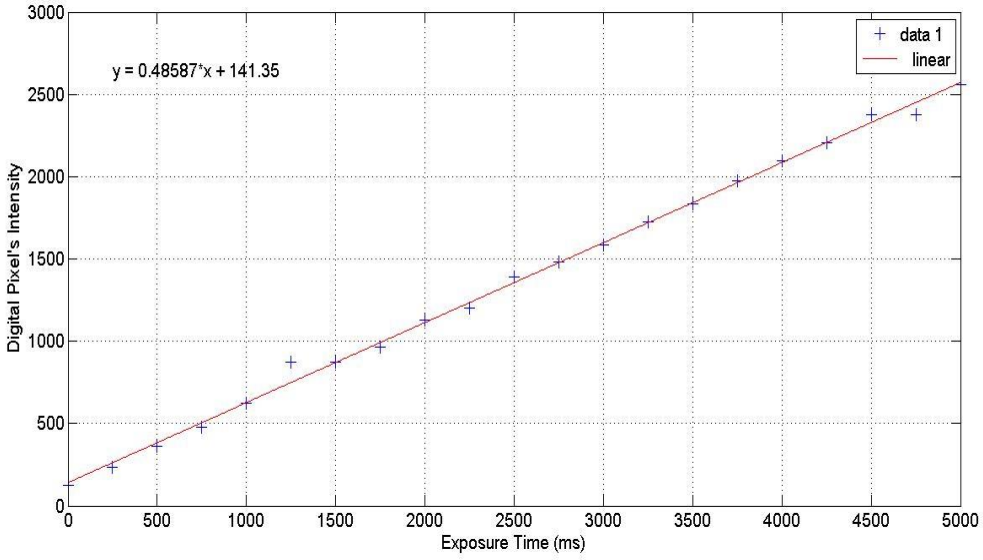

Figure II.16 Linearity test for the CCD camera at (100, 1292) pixel's location of (1040 x 1392) pixel image

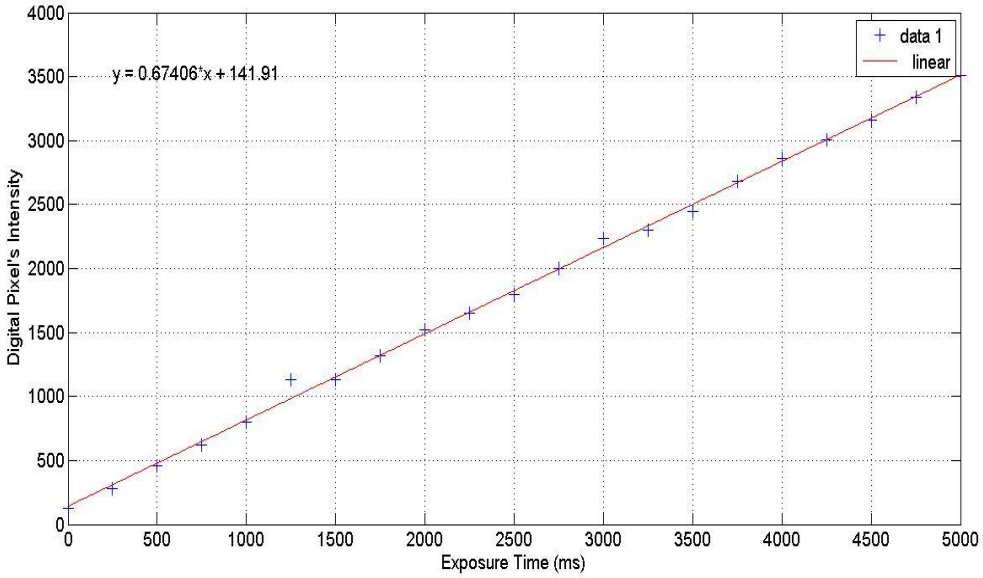

Figure II.17 Linearity test for the CCD camera at (520, 696) pixel's location of (1040 x 1392) pixel image

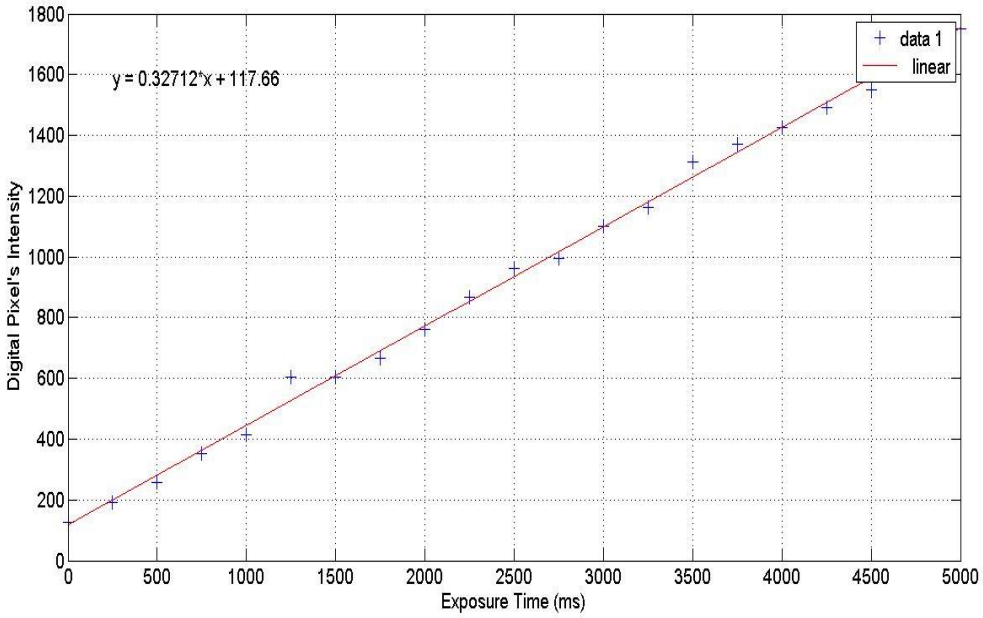

Figure II.18 Linearity test for the CCD camera at (940, 100) pixel's location of (1040 x 1392) pixel image

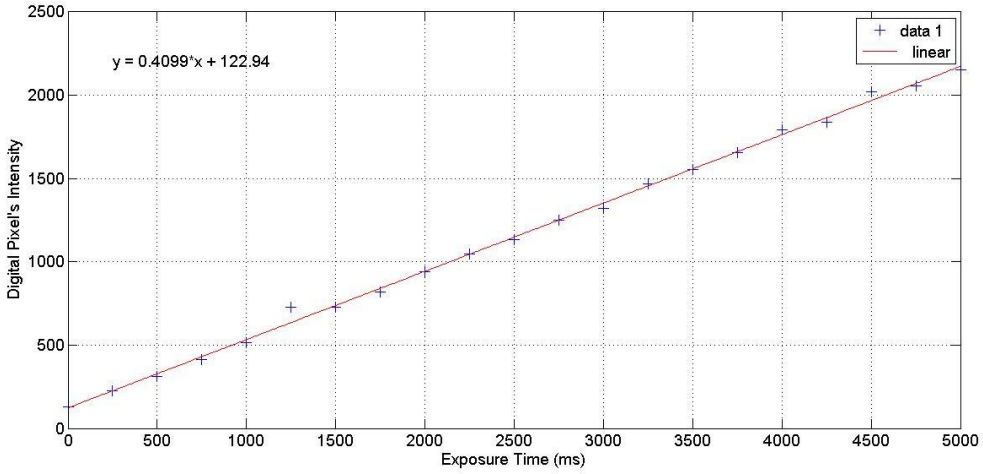

Figure II.19 Linearity test for the CCD camera at (940, 1292) pixel's location of (1040 x 1392) pixel image

Sample Preparation

Another significant and vital part before initiating these experiments is the case study sample preparation. This operation has had a lot of impacts on the results, on the whole, and during the course of action through conducting these experiments. This process is started by getting the animal down, decapitated, after being briefly anesthetized via isoflurane inhalation (IsoFlo, Abbott Laboratories, USA). All animals that are allocated for those sets of experiments were six to eight weeks old mice from which coronal and sagittal brain slices were prepared. Then the brain is being taken out of the skull through a neat procedure and was dissected out under ice-cold dissection Ringer containing either (in mM): Ringer 1: 125 NaCl, 2.5 KCl, 1 $MgCl_2$, 0.1 $CaCl_2$, 25 glucose, 1.25 NaH_2PO_4, 25 $NaHCO_3$, 0.4 ascorbic acid, 3 myo-inositol, and 2 pyruvic acid; or Ringer 2: 200 sucrose, 1.25 NaH_2PO_4, 26 $NaHCO_3$, 10 glucose, 3.5 KCl, 7 MgCl, 1.5 ascorbic acid (all chemicals from Sigma). After that, it's adhered and sliced using the

slicing machine to different slices thicknesses (mainly 600 µm). Those slices were cut with a vibratome (VT1000S, Leica), transferred to an incubation chamber containing extracellular solution (ECS) [ECS; containing (in mM) 125 NaCl, 2.5 KCl, 1 $MgCl_2$, 2 $CaCl_2$, 25 glucose, 1.25 NaH_2PO_4, 25 $NaHCO_3$, 0.4 ascorbic acid, 3 myo-inositol, and 2 pyruvic acid, all chemicals from Sigma] and bubbled with 5% CO_2-95% O_2. Slices were incubated in ECS for 15 – 30 minutes at 37ºC and then cooled down to room temperature. All measurements were obtained within 2–3 h of slicing.

Targeted Brain Areas

The brain areas that have been dealt with throughout this study are: Medial Nucleus of the Trapezoid Body (MNTB), Ventral Nucleus of the Trapezoid Body (VNTB), Lateral Superior Olive (LSO), Pedunculopontine Tegmental nucleus (PPT), Superior Colliculus (SC), Cornu Ammonis 3 of hippocampus (CA3), the cerebellar cortex molecular layer, Olfactory Bulb (OB). The brain regions were chosen because previous knowledge suggested that they would represent a wide range of scattering coefficients, but also to perform control experiments for future optogenetics manipulations.

And since in these experiments, the thicknesses of the samples play a significant role in determining how the results would look like, this issue has been always borne in mind and taken into account by having those brain areas completely confined within the sample thickness, by making its surface as a flat as it could be, and by immersing it in the ECS while doing the slicing process and when the measurements are being taken. Moreover, sometimes it's also being bubbled throughout the experiment to keep it oxygenated. The truth of the matter behind these strict sample preparations is the

tendency to mimic almost the same "in vivo" environment and maintain the metabolism of the sample as long as possible. This study has shown how this aspect has an absolute relevance with how those biological tissues respond optically (more details will be presented in the discussion section).

Experimental Procedure

Manually-Controlled Method

After the sample is prepared with a certain thickness, it is transferred to a small chamber that is transparent from the bottom to make it more convenient for using with the inverted microscope. That chamber will have been already cleaned using special lens papers. The sample will be floating inside the preserving fluid (that is bubbled sometimes to keep it oxygenated and healthy, as it is mentioned before). And for that reason, it is required to add a piece of metal with strings as a mass to keep it from that random movement. However, the latter has undesirable effects on the sample as well; these effects will be elucidated in the discussion section. The earlier stages of these sets of experiments had been done manually without having a pico-motor and the CCD video camera and the monitor, by trying to land the fiber tip on the top of the sample and get it to be centered on the targeted area without forgetting having the sample being in focus by moving the stage up and down, and take an image that represents arbitrary digital intensities for the original optical power intensities after passing through that specific thickness. Then, that sample will be replaced by another one with another thickness and the same procedure is being repeated. The current intensity that is corresponding to the aimed optical power intensity is set up based on the optical power intensities curves for

each individual optical fiber. Room's lights will be turned off to avoid any other illumination sources. The main goal for those types of experiments was to construct a curve for the arbitrary digital intensities or the optical power intensities as a function of sample thickness. Each point accounts for the maximum intensity accompanied with the fact that this fiber optic output profile is Gaussian (Some results belongs to this approach can be seen in figure II.20).

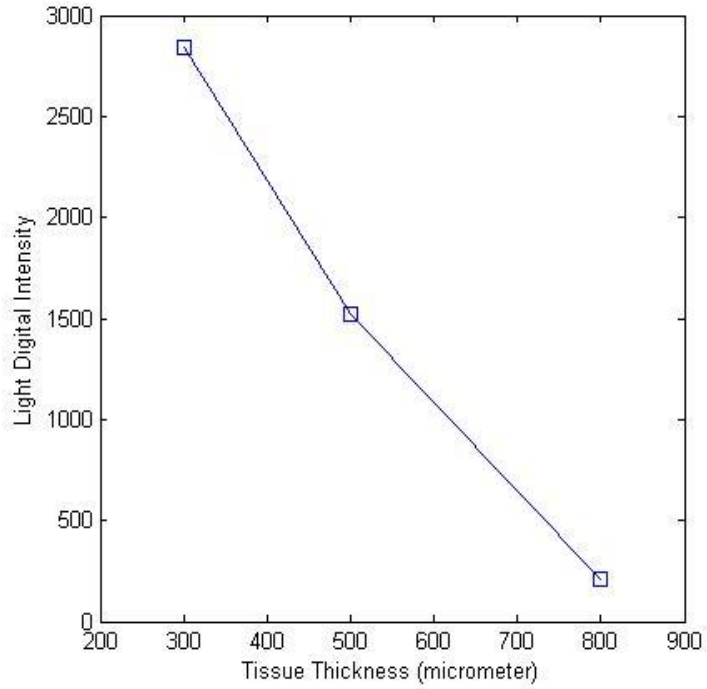

Figure II.20 Light arbitrary digital intensity as a function of tissue's thickness for a PPT region. This is a one single set of measurements

As it stated earlier, the first sets of experiments had been performed without having the pico-motor which is implemented later in order to make punching through the brain's samples possible with higher accuracy (see next section). Before that, all the punching trials had been done manually which had been considered to be a vague process since there are no enough clues to determine how far the fiber tip inside the sample goes.

Pico-Motor-Controlled Fiber Punch-Through Method

The other approach that has been launched after that pico-motor and the CCD video camera had been installed to the system is the punching through approach or "fiber punch-through method". In this approach, instead of having several samples with different thicknesses in order to construct that formerly mentioned graph, there will be only one sample with the thickness that contained the whole area under investigation from the top to the bottom, and now the fiber tip can punch through driven by that pico-motor through precisely determined step sizes to trace the total moving distance after making sure that the fiber tip is properly landed on the top of the sample surface.

After the incubation period, a slice was placed into a measurement chamber and continuously superfused with bubbled extracellular solution for the duration of the experiment. The measurement chamber was then positioned on the inverted microscope in which the standard transmitted light source was replaced by an assembly consisting of a three-axis manual micromanipulator (Narishige model MM-3), a calibrated piezo driven one axis micromanipulator (Model 8302 Picomotor Actuator, Newport, Irvine, CA), and a custom made optical fiber holder to hold one of the three fiber/LED assemblies in place. The output end of the optical fiber was placed directly onto the surface of the brain slice under the guidance of the CCD video camera using macro optics, such that the emitted light was facing the brain section and the microscope's objective (EF 10x, N.A. 0.25, Leitz Wetzlar, Germany). The light was then captured by the monochromatic 12bit camera attached to the microscope via the camera port (see figure II.21 for a sketch of the setup).

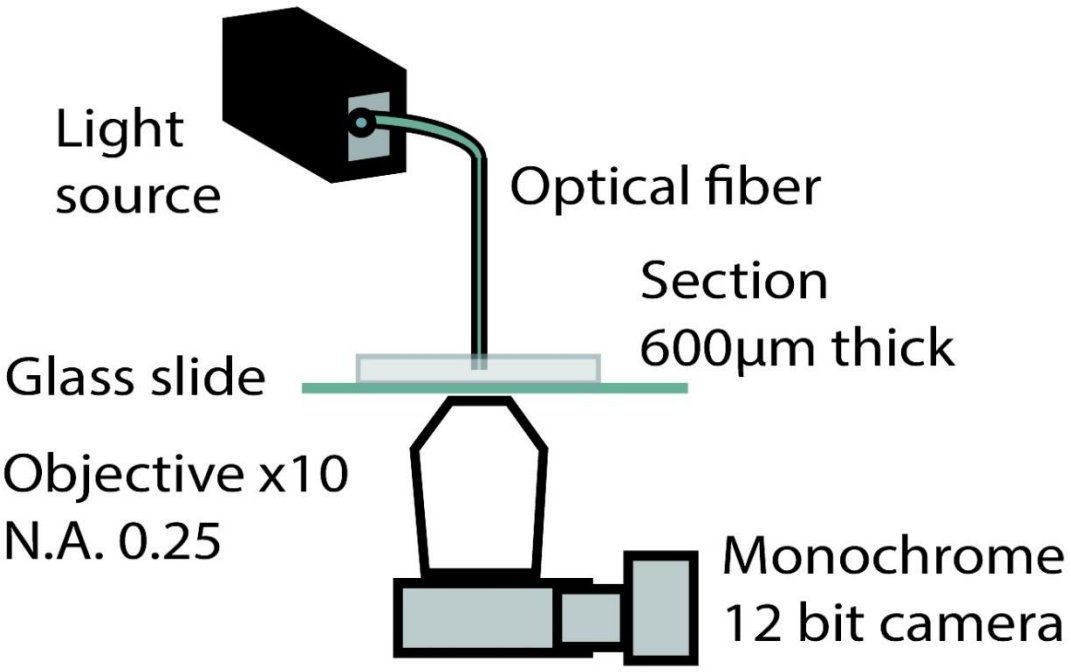

Figure II.21 Basic experimental setup of the punch-through method. On an inverted microscope, an optical fiber was placed on a section of brain tissue such that light from the fiber would pass through the tissue and subsequently be imaged by an objective attached to a CCD camera [12]

Exposure time and the irradiance of the optical fiber (I_o) were adjusted to optimally utilize the Mightex camera dynamic range throughout the entire data set. Subsequently, the fiber was lowered into the slice in 5 µm steps using the precision piezo micromanipulator, starting from the surface of the section and ending at a depth of 500 µm. At every step, the camera will be taking a number of images and get them to be averaged by a number, which can be manipulated from the controlling program front panel. Instantaneously, a graph will be drawn for arbitrary digital intensities as a function of sample thickness after allocating the cursor in the right position. Consequently, the images taken will be stored in a chosen folder to pave the way for more data analysis to be accomplished upon them succeedingly.

Computer software, LabVIEW 2009 Service Pack 1 (National Instruments, Austin, TX), has been installed on the computer, and a computer program was written in this software to control the pico-motor and get it to move up and down in very precise step sizes, and to control the Mightex camera. Other very important parameters can be changed or adjusted through the program panel; for example, the CCD camera exposure time, total moving distance, the number of pictures that are going to be taken and averaged for each individual step size measurement. It is also allowed to change the cursor position to another pixel location rather than the central one to read the digital intensities from those pixels locations (a snap shot for the controlling program front panel screen can be seen in figure II.22).

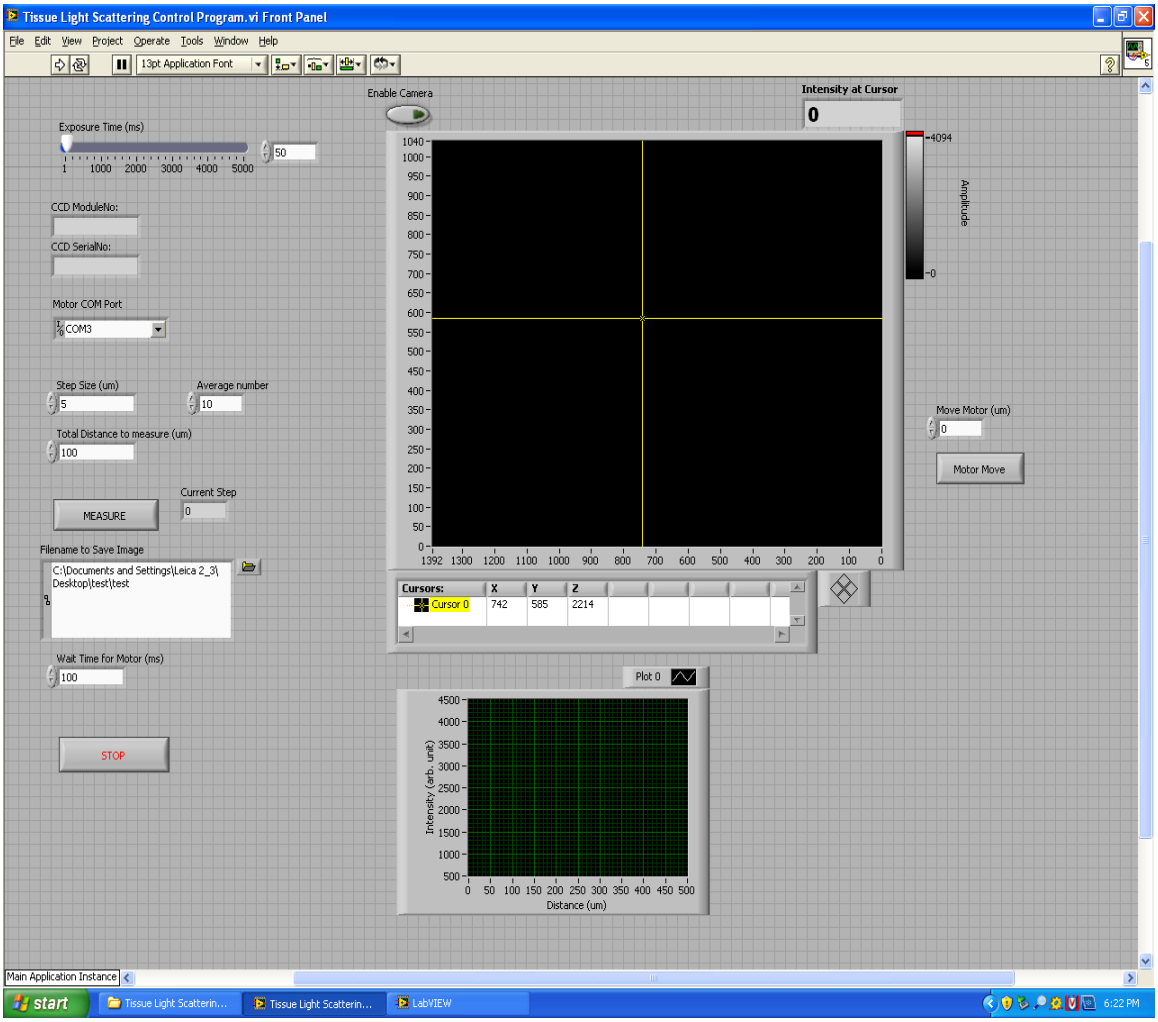

Figure II.22 A snap shot for the controlling program front panel expressing the adjustable significant parameters and other details

Images taken at different steps were stored for further data analysis. An example of such an image is shown in figure II.23.

Figure II.23 An example of an original image captured by the CCD camera, showing light emitted from an optical fiber after it passed though a section of brain tissue [12]

The data was extracted from images by locating the pixel representing the fiber center, and collecting that pixel 12 bit gray scale value for the digitized optical irradiance $I(z)$. This process was repeated for each image. $I(z)$ was normalized to I_o to obtain the optical transmittance $T(z) = I(z)/I_o$, which was then fitted by a single exponential function (Figure II.24) according to the modified Beer-lambert law (see Chapter III) to extract the effective attenuation coefficient μ_{eff} of the measured neural target.

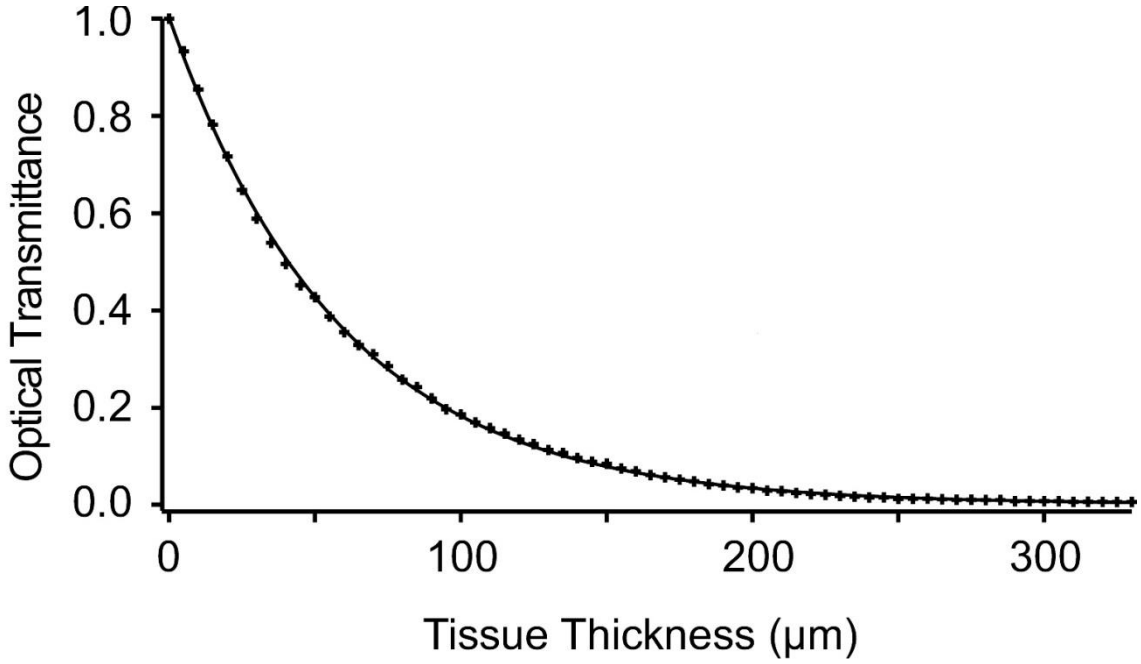

Figure II.24 Optical transmittance as a function of tissue thickness. As the optical fiber was advanced through the section of brain tissue and repeated images such as the one in figure II.23 were taken, the decrease in optical transmittance as a function of tissue thickness could be evaluated. The single measurements ("+" symbols) represent transmittance of blue light (453 nm) through a section of PPT at various thicknesses, while the solid line represents an exponential fit [12]

Eventually, the output optical power intensity and the light profile will be tested again to be certain that the fiber tip has not been defected and the light profile is not distorted throughout the experiment.

Control experiments determined that the forces applied on the tissue by the advancing glass fiber are comparable to those created by an advancing sharp microelectrode (< 200 μN, data not shown). We thus concluded that lowering the fiber into the tissue caused the fiber tip to slice through, rather than squish the tissue together, such that measurements at many different tissue thicknesses could be taken reliably from the same tissue section at precisely controlled depths (referred to as "fiber punch-through method").

Light Profile and Tissue Damage Control Experiments

Incidentally, and as it is referred to the idea of whether the light profile is enough to cover the targeted areas or not, it is convenient to show the results regarding this part of the study as shown in figure II.25.

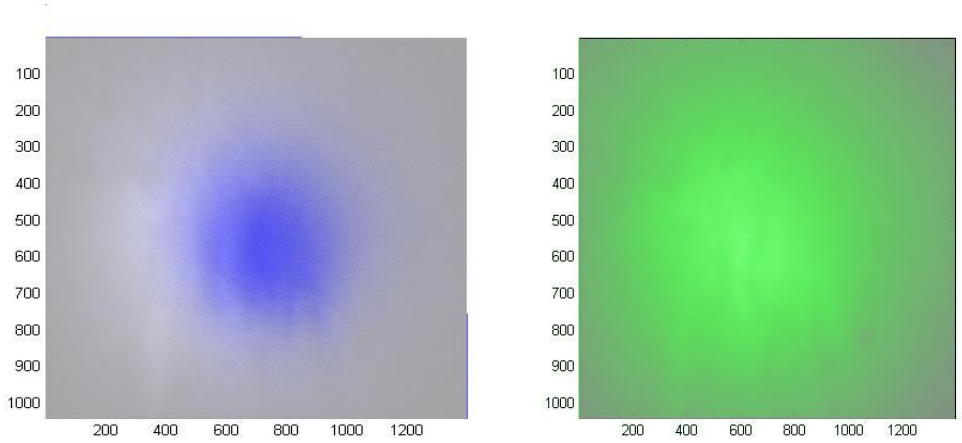

Figure II.25 (Left) it is an overlapped picture of two images that are taken for a PPT region, in 300 µm of thickness and 1300 µm from the midline of depth slide. The background image (which is in black and white colors) shows the PPT area, while the blue one is, the output optical power intensity profile for the 100 µm core optical fiber connected to a 453 nm blue LED, driven by a 28 mA current source. This picture is evidence that the blue LED light is not sufficient to cover the whole PPT region. These two images are taken on an integration time of 100 ms. (Right) it is an overlapped picture of two images that are taken for a PPT region, in 300 µm of thickness and 1300 µm from the midline of depth slide. The background image (which is in black and white colors) shows the PPT area, while the green one is, the output optical power intensity profile for the 100 µm core optical fiber connected to a 518 nm green LED, driven by a 100 mA current source. This picture is evidence that the green LED light is not sufficient to cover the whole PPT region. These two images are taken on an integration time of 100 ms

Another potential trial which has emerged from the eagerness of showing how the laser light intensity could expose a thermal damage in the targeted area had been performed and its results are nicely presented in figure II.26.

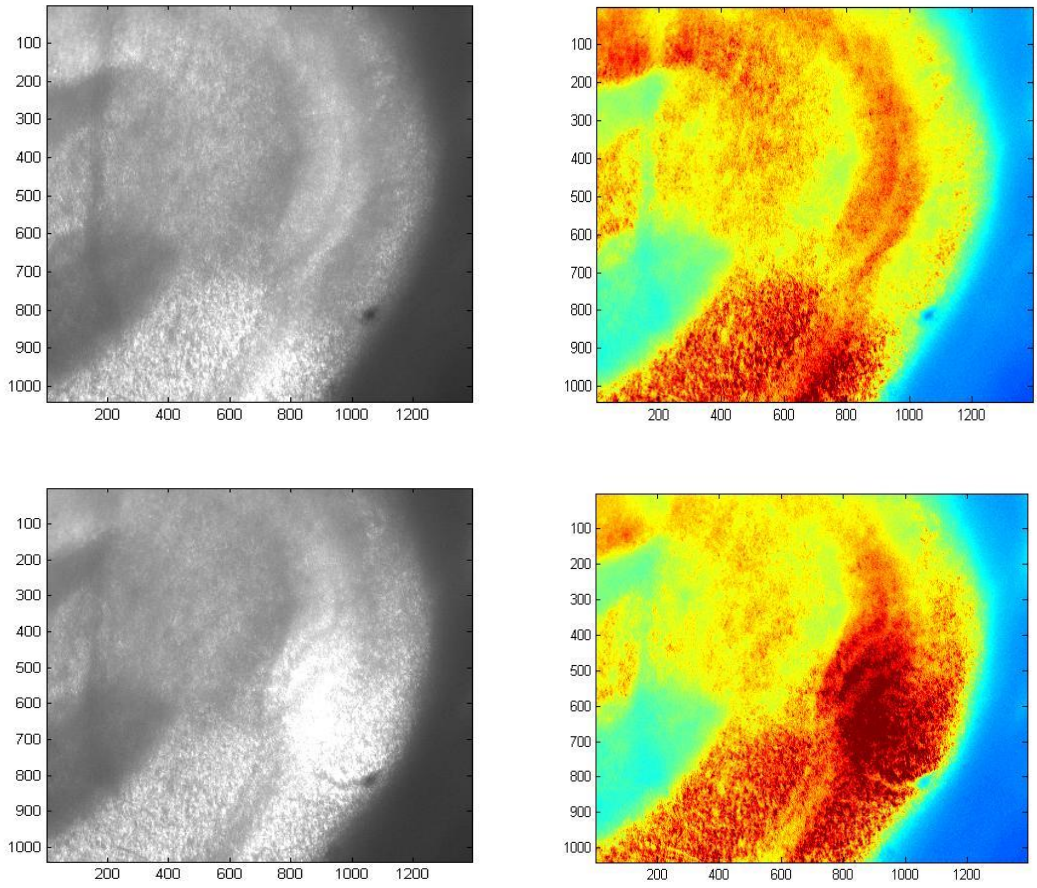

Figure II.26 (Top left) a 300 µm of thickness and a 1500 µm from the midline of depth slide's image, showing the actual image that is taken from the CCD camera, of the CA3 Hippocampus region under white light illumination and before the laser damage. This image is taken on an integration time of 100 ms. (Top right) a 300 µm of thickness and a 1500 µm from the midline of depth slide's image, showing the false color of the CA3 Hippocampus region under white light illumination and before the laser damage. This image is taken on an integration time of 100 ms. (Bottom left) a 300 µm of thickness and a 1500 µm from the midline of depth slide's image, showing the actual image, that is taken from the CCD camera, of the CA3 Hippocampus region under 405 nm and 3.5 mW laser source illumination, being applied for 3 minutes of time. The image shows a real tissue damage which is caused by the laser source under these circumstances. This image is taken on an integration time of 100 ms. (Bottom right) A 300 µm of thickness and a 1500 µm from the midline of depth slide's image, showing the false color of the CA3 Hippocampus region under 405 nm and 3.5 mW laser source illumination, being applied for 3 minutes of time. The image shows a real tissue damage which is caused by the laser source under these circumstances. This image is taken on an integration time of 100 ms

Now that, tissue damage was checked. Therefore, it was concluded that it needs to illuminate the section with much higher light intensities and exposure times to cause damage than what has been used during this study measurements.

CHAPTER III

DATA ANALYSES, THE MODIFIED BEER-LAMBERT LAW, BRAIN ATLAS ESTABLISHMENT, AND RESULTS

Data Analyses

The results associated with this study are strictly taken from the following brain areas: MNTB, VNTB, LSO, PPT, SC, CA3, and Cerebellum. Although the images have been stored, yet they are still considered to be raw data and it is required to make it through a series of data analysis steps before they can be scientifically illustrated corresponding to multi-data presentations that serve to answer the fundamental questions and aims of this study.

The results could be introduced by following these steps: the pre-stored images in a specific folder are reloaded to another viewer program that is programmed in LabVIEW software as well, that allows retrieving the intensities from those images according to a cursor location that is also adjustable by the analyzer. Then, these intensities that are corresponding to each tissue thickness will be saved in an appropriate format. This process still be pursued by a sorting one and thereby, they are ready to be depicted now. A snap shot for the viewer program is illustrated in figure III.1.

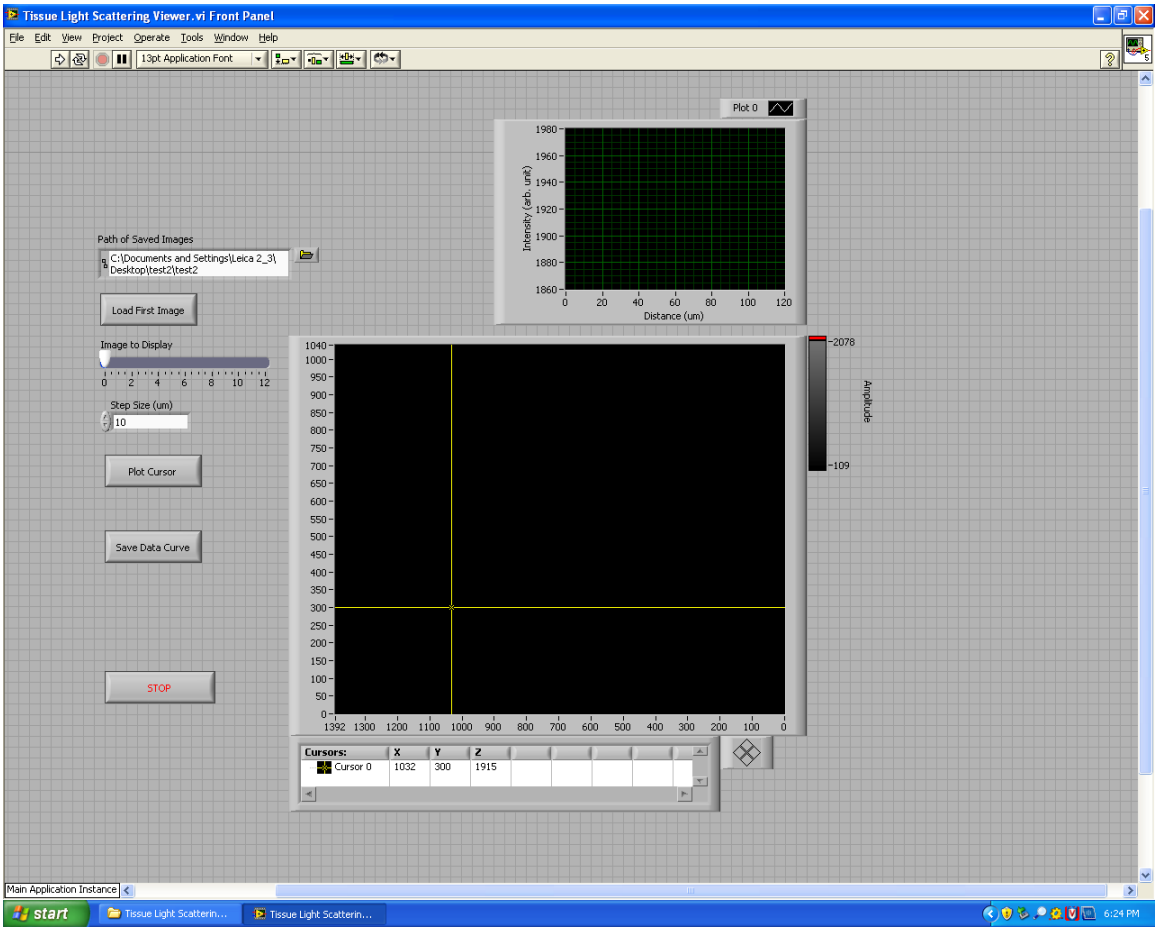

Figure III.1 A snap shot for the viewer program front panel screen that is used for retrieving the intensities from the images and plotting them as a function of tissue thickness according to the specific cursor location

Two programs that have been used in order to graph the resultant data are: MATLAB R2010a and Igor 6. That resulted curves are normalized so that they are in a comparable forms. It is of fundamental importance that these data are being fitted with the most suitable equation form to make it possible to extract some valuable parameters like the one mentioned sooner- the effective attenuation coefficient (μ_t) that belongs to each region under investigation. The first equation that had been used to fit the data was

the modified Beer-Lambert law for light scattering and absorption in biological tissues, which has the form of:

$$I(x) = I_o e^{-\mu_t x}$$

In which:

$I(x)$: is the optical power intensity as a function of tissue thickness (mW/mm^2)

I_o: is the initial optical power intensity (mW/mm^2) (when x=0 mm)

μ_t: is the effective attenuation coefficient (1/mm)

x: is the tissue thickness (mm)

More elaborate theoretical background pertaining to the modified Beer-Lambert law is presented in the following section.

Some of the results that had adopted this approach are shown in the figures III.4-6 using MATLAB. In these figures, the “one” and “two” words refer to the first and second measurements on the first and second slices used in that experiment, respectively. A full comprehensive description for the experiment that the following figures have been based on is elucidated as follows:

In this experiment, a 600 µm thick slice is used and punched through different depth following the multiple different step-sizes of the motor (5 µm step-size are used). The total moving distance was 500 µm in depth making the smallest thickness taking into our consideration to be 100 µm. The optical source used in this experiment is a blue LED light (453 nm) coupled to a 100 µm core diameter optical fiber with an output power of 4.33 mW/mm^2 from this fiber. The LED source is driven by a 28 mA current to get this power. The CCD camera was set on 50 ms exposure time throughout the experiment.

The aims of these data analyses are to extract the pixels' digital intensities from the images taken. Then, get rid of the saturation values. After that, the raw data are drawn and their exponential curves are obtained. These raw data and fitting curves are normalized, as well, in order to make the results comparable to each other properly.

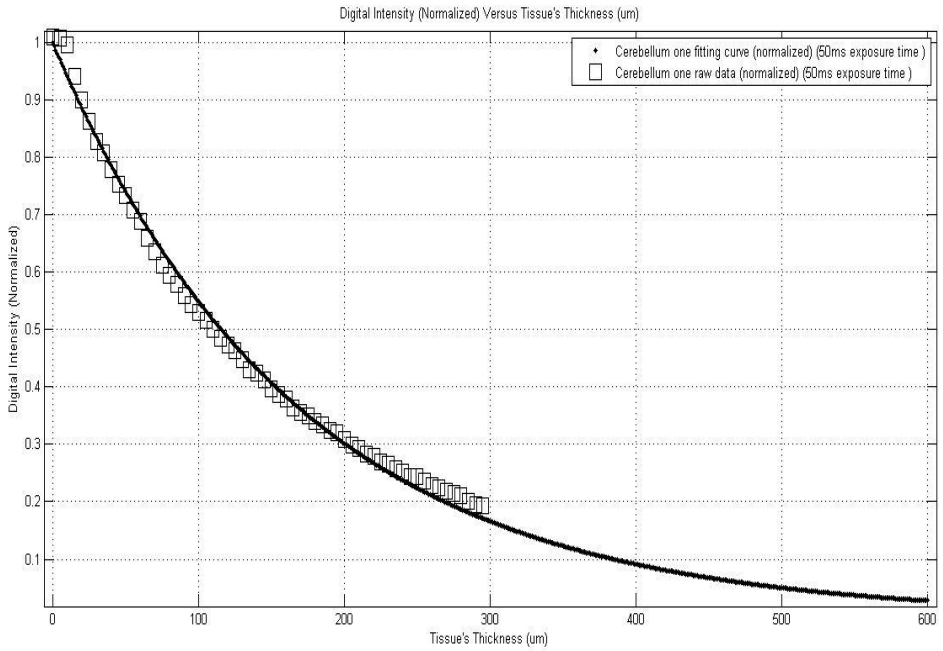

Figure III.2 A cerebellum one raw data and fitting curve. Note the offset in the fit. This issue will be addressed below

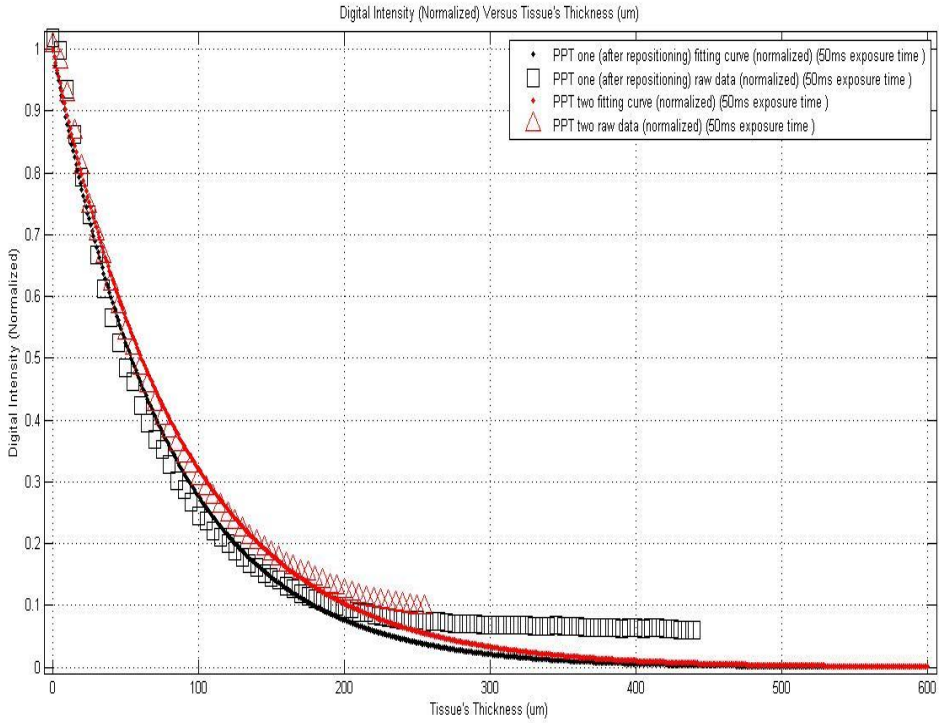

Figure III.3 A comparison between PPT one and PPT two. Note the offset in the fit. This issue will be addressed below

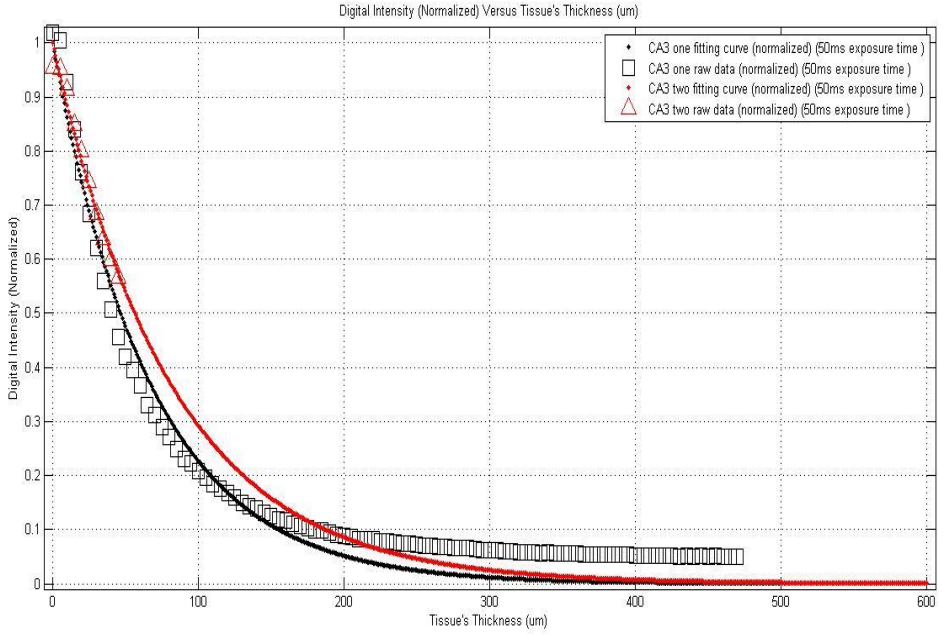

Figure III.4 A comparison between CA3 one and CA3 two. Note the offset in the fit. This issue will be addressed below

The obtained data follows an exponentially decaying curve as predicted by the modified Beer-Lambert law. However, due to the electronic offset and other optical background, there is an artificial offset needed to be accounted in the data. Having taken that into account, the new fitting equation, for now, looks like the following:

$$I(x) = Y_o + I_o e^{-\mu_t x}$$

One can simply see that this equation is of the same format as the old one with only one term added to it which is Y_o which refers to that initial intensity. Thus, the same data reanalyzed applying the latter approach and this time using Igor programming, and the results are demonstrated in the following figures (Figure III.5 and Figure III.6). It is also important to indicate that "Tau" in these figures accounts for the effective attenuation coefficients.

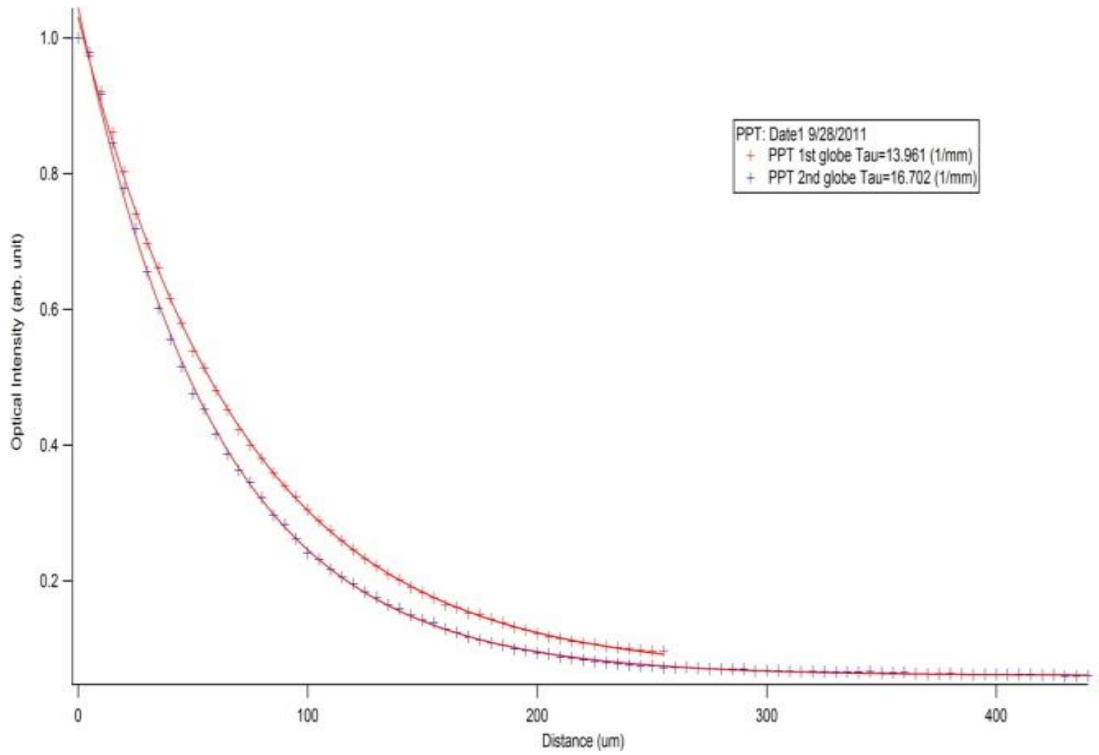

Figure III.5 A comparison between PPT one and PPT two after taking the offset factor Y_o into account which demonstrates its significant impact on the reanalyzed and refitted the data

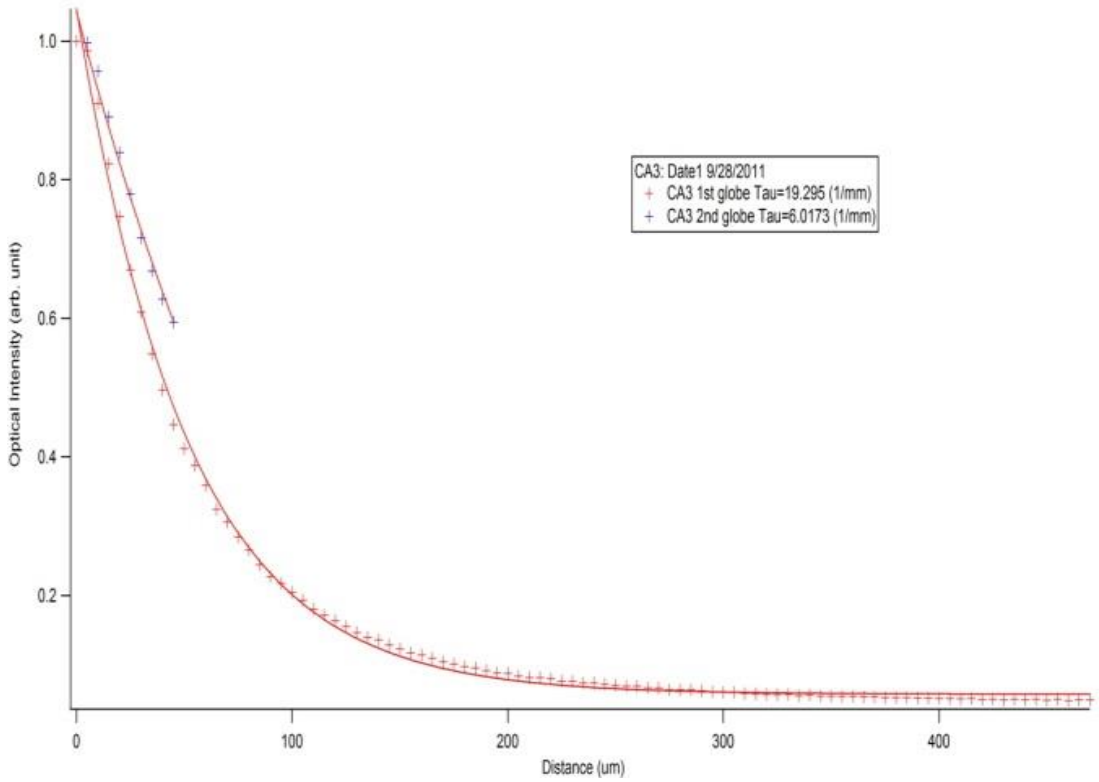

Figure III.6 A comparison between CA3 one and CA3 two after taking the offset factor Y_o into account which demonstrates its significant impact on the reanalyzed and refitted the data

The Modified Beer-Lambert Law and the Effective Attenuation Coefficients for Highly Scattering Neural Targets

The full mathematical treatment of light travelling in biological tissue that absorbs and scatters light-waves (or optical photons) is described by the Radiative Transport Equation (RTE) [13], [14].

$$\frac{1}{c}\frac{\partial L(\vec{r},\hat{s},t)}{\partial t}+\hat{s}\cdot\nabla L(\vec{r},\hat{s},t)+(\mu_a+\mu_s)L(\vec{r},\hat{s},t)-\mu_s\int_0^{4\pi}L(\vec{r},\hat{s},t)P(\hat{s}'\cdot\hat{s})d\Omega'=S(\vec{r},\hat{s},t)$$

Where $L(\vec{r},\hat{s},t)$ is the radiance ($W\ m^{-2}sr^{-1}$) of the propagating light-wave; μ_a and μ_s are the absorption, scattering coefficients (m^{-1}) of the biological tissue; $P(\hat{s}'\cdot\hat{s})$

is the phase function describing the probability of a photon scattered to the radiation direction $\hat{s}'$ from its original radiation direction $\hat{s}$; $S(\vec{r},\hat{s},t)$ is the optical energy density ($W\,m^{-3}sr^{-1}$) generated in the biological tissue; c is the speed of light in vacuum and Ω is the solid angle.

The RTE is a complex equation which has no analytical solution, since $L(\vec{r},\hat{s},t)$ depends on both the spatial coordinate ($\vec{r}$) and the radiation direction ($\hat{s}$) and time (t), resulting in a function with seven independent variables. $L(\vec{r},\hat{s},t)$ can be evaluated computationally with the RTE but requires an involved computational algorithm such as a Monte-Carlo stochastic simulation [15], [16]. Therefore, to extract quantitative parameters from our empirical measurements, a simplification of the RTE is needed. For most biological samples, including the brain, the scattering coefficient at the wavelengths tested here is typically one to two orders of magnitude higher than the absorption coefficient ($\mu_s \gg \mu_a$). In addition, the phase function $P(\hat{s}'\cdot\hat{s})$ can be approximated by the Heyney-Greenstein function [17]:

$$P(\hat{s}'\cdot\hat{s}) \equiv P(\cos\theta) = \frac{1-g^2}{2(1+g^2-2g\cos\theta)^{3/2}}$$

Where g is the anisotropy factor and is generally assumed to be larger than ~0.9 ($0.9 \le g \le 1$) in most biological tissues, indicating that the scattering light is predominantly forward-scattered. Under these conditions, the RTE can be approximated by the diffusion equation (the details of the simplification can be found in [13]:

$$\frac{1}{c}\frac{\partial I(\vec{r},t)}{\partial t} + \mu_a I(\vec{r},t) - \frac{1}{3[\mu_a + \mu_s(1-g)]}\nabla^2 I(\vec{r},t) = S(\vec{r},t)$$

Where $I(\vec{r},t) = \int_0^{4\pi} L(\vec{r},\hat{s},t)d\Omega$ is the irradiance ($W\ m^{-2}$), or in the laboratory commonly (but erroneously) called intensity of the light wave, and $S(\vec{r},t) = 4\pi \int_0^{4\pi} S(\vec{r},\hat{s},t)d\Omega$. To further simply the diffusion equation, we further assume that the optical propagation is in a steady-state condition ($\partial I(\vec{r},t)/\partial t = 0$) and there is no light being generated in the biological tissue $S(\vec{r},t) = 0$. Therefore, the 1D diffusion equation can simply be written as a 1D second-order differential equation [14]:

$$\frac{d^2 I(z)}{dz^2} = \mu_{eff}^2 I(z)$$

Where $\mu_{eff} = \sqrt{3\mu_a[\mu_a + \mu_s(1-g)]}$ is the effective attenuation coefficient. Hence, the solution of the 1D diffusion equation is the modified Beer-Lambert Law [14]:

$$\frac{I(z)}{I_0} \equiv T(z) = \exp(-\mu_{eff} z)$$

With I_o being the irradiance measured at the fiber output of the optical fiber, and z being the longitudinal distance from the fiber output. The ratio of $I(z)$ against I_o is the optical transmittance $T(z)$ which follows an exponential decay against the longitudinal distance z. In this study, we attempt to estimate the optical penetration depth within a brain nucleus to determine optical fiber source excitation efficacy of the opsin expressed within this neural target. It is clear from the above equation that it is not necessary –at the three wavelengths tested hereto individually measure μ_a, μ_s and g. Rather, simply measuring the effective attenuation coefficient μ_{eff} is sufficient for this estimation.

The Brain Atlas, and a Technique of Mapping the Effective Attenuation Coefficients across the Entire Brain

The technique of using an optical fiber to punch through a brain slice allows collecting data from well identified brain areas at very precise depths. However, it would be impractical to use this technique to map the effective attenuation coefficients $\mu_{eff}(\vec{r})$ of many (i.e. hundreds) of brain areas, which would be required to obtain a quantitative picture across the entire brain. However, imaging brain slices using bright-field light transmission microscopy with monochromatic light and combining these images with the measured effective attenuation coefficients obtained from the punch-through method on selected neural targets allowed us to calculate and map out the effective attenuation coefficients across the entire brain. Whole brain slice imaging was performed on an Olympus VS 120 microscope, using transmitted light filtered via 546 /20 nm band-pass filter and a 10x (N.A. 0.40) objective. To allow seamless, quantitatively correct tiling of multiple images of a single brain section, the manufacturer calibrated the microscope to normalize for uniform illumination and data acquisition across the entire imaging area. With this normalization, the illumination irradiance I_o can be assumed to be a constant across the whole brain slice scan.

The illumination irradiance I_o of the microscope is difficult to measure directly, instead brain slices containing the brain areas measured previously with the punch-through method were used to quantify and normalize I_o. For a previously measured brain area, using the modified Beer-Lambert law, the illumination irradiance I_o can be estimated by

$$I_o = \frac{I(x_o, y_o, z_o)}{\exp\left[-\mu_{eff}(x_o, y_o) \cdot z_o\right]}$$

Effective attenuation coefficients $\mu_{eff}(x, y)$ of other brain areas not measured with the punch-through method can subsequently be calculated using

$$\mu_{eff}(x, y) = -\frac{1}{z_o} \log_e[\frac{I(x, y, z_o)}{I_o}]$$

The Effective Excitation Distance for Optogenetic Proteins

In optogenetic experiments, it is important to estimate the minimum optical irradiance required to effectively excite the desired neural area longitudinally to maximize excitation of the optogenetic proteins. Assuming the minimum excitation irradiance threshold for an optogenetic protein is I_{min} and the irradiance at the fiber output is I_{fiber}, the effective excitation distance d in the longitudinal direction of a neural target, which has an effective attenuation coefficient of μ_{eff} can be calculated by the following equation

$$d = -\frac{1}{\mu_{eff}} \log_e[\frac{I_{min}}{I_{fiber}}]$$

Integration of All Relevant Data in a Computer Program

From a practical point of view, an investigator wishing to perform optogenetic manipulations *in-vivo* in the brain area of his/her choice needs to be able to estimate the required light intensity that needs to be fed into an optical fiber to obtain optimal illumination of the brain area to be manipulated. A situation where too much light energy is used may result in tissue damage and is therefore undesirable. Furthermore, feeding too much light energy into an optical fiber may result in unspecific activation of optogenetic

proteins outside the intended brain area, potentially compromising the experimental design. On the other hand, in a situation where not enough light energy is used, optogenetic proteins will fail to be activated. To aid with determining the correct amount of light energy for a given experimental situation, we prepared a brain atlas that maps effective attenuation coefficients across the entire mouse brain. This atlas is integrated into a computer program that an investigator may use to estimate the required amount of light energy for an individual experimental situation based on brain area, desired penetration depth, and light frequency used. For further information, see www.optogeneticsapp.com.

Results

The main goal of this study was to test the hypothesis that different brain neural targets scatter light differently, and that these differences are significantly large such that they need to be considered for successful optogenetic activation in deep brain nuclei. A secondary goal was to establish a database of light scattering values for different regions of the mouse brain that could be used as a reference in future experiments in which illumination of neural tissue is required. The most common approach to bring light into deep brain areas *invivo* is via optical fibers that are stereotactically placed above the brain area of interest. Our experimental approach of advancing a light emitting optical fiber through brain tissue modeled such a situation well, and enabled us to precisely determine light intensity at any depth along the longitudinal axis with respect to the fiber tip.

Light Intensity Decreases Exponentially in Brain Tissue

An acute brain slice was placed into a perfusion chamber under an inverted microscope, and an optical fiber attached to a LED was placed directly on the tissue surface. Light emitted from this fiber propagated through the slice and was then collected by the objective and the chip of the attached monochromatic camera. A sketch of this configuration is shown in figure II.21, and an example of an original image acquired with this setup is shown in figure II.23. This configuration of imaging the light emitted from an optical fiber tip after it passed through a piece of brain tissue of known origin and of a known thickness d allowed effective measurement of the remaining light intensity at tissue depth d. From this value we could then calculate the ratio of the intensity of remaining light at depth d over the original light intensity at the optical fiber tip.

Subsequently, the optical fiber was lowered into the section in 5 μm steps, and similar images were acquired with each step. Control experiments verified that advancing the fiber into the tissue caused it to reliably slice through the section rather than compress the section (data not shown). Advancing the fiber into the tissue (referred to as the "fiber punch-through method"), and taking repeated images at various depths effectively created a dataset of light intensity measurements in brain tissue at points progressively closer to the fiber tip. An alternative approach would have been to cut brain slices of different thicknesses and measuring light transmitted through each one of these slices. However, the fiber punch-through method allowed us to control for tissue depth (thickness) much more precisely than cutting sections of various thicknesses would have allowed us to do, and furthermore allowed us to measure the *exact* same piece of tissue at different depths.

From the measurements obtained at various tissue depths, light intensity ratios were calculated and plotted. Curve fitting indicated that the data points were best described by a single exponential function. An example of such a fit is shown in figure II.24, representing a set of measurements with blue light (453 nm) recorded from a section of PPT. The '+' symbols represent the measured luminance at each tissue thickness, and the superimposed line represents the exponential fit.

Light Scattering Properties Vary across Different Brain Regions

Eight different brain regions were measured with 453 nm light in the same way as the PPT shown before (Figure III.7). The data points (colored symbols) were plotted against the distance from the fiber tip, and the set of measurements from each brain area were fitted with a single exponential function (colored lines).

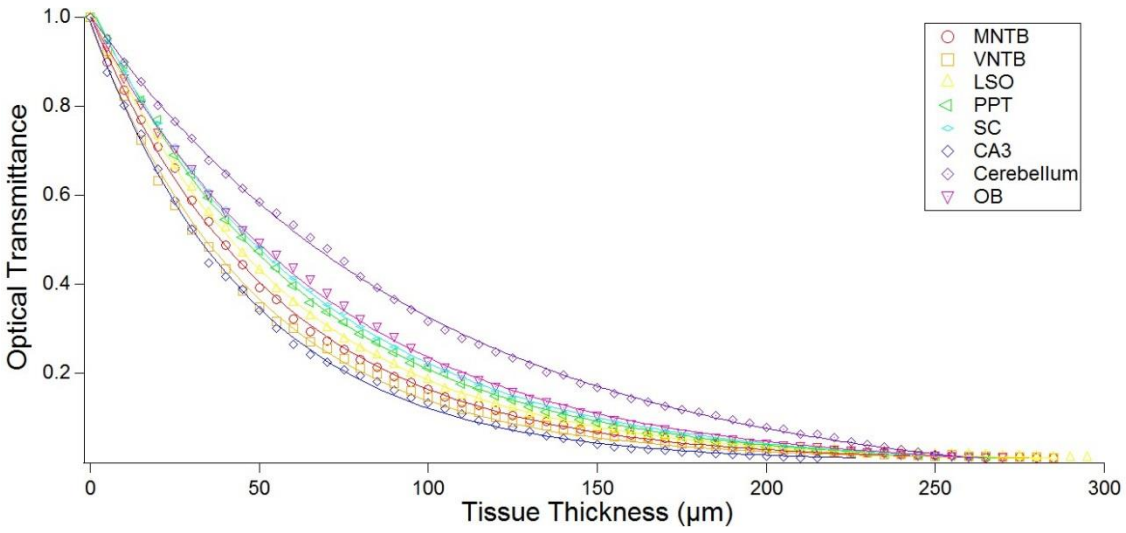

Figure III.7 Optical transmittance through different types of brain tissue. Measurements using the fiber punch-through technique were taken in eight different brain areas with blue (453 nm) light. In each case, optical transmittance decreased exponentially with tissue thickness; however, the exponential decreases observed varied greatly with the type of tissue. Single measurements are represented by the respective symbols while the solid lines represent exponential fits of the data

The results indicate that light intensity dropped at least 10-fold within a 200 µm distance from the tip of the optical fiber in each brain region tested. Importantly, the data suggest that this drop differs substantially among the brain regions tested. To systematically examine these differences, we calculated scattering coefficients from the data (Figure III.8). Average coefficients ranged from 19.96 +/- 0.26 for VNTB tissue, representing the lowest light transmittance of any region tested, to 9.76 +/- 0.78 for cerebellum, representing the highest transparency of all brain regions tested. For all values and SEMs, see figure III.8 and corresponding figure caption.

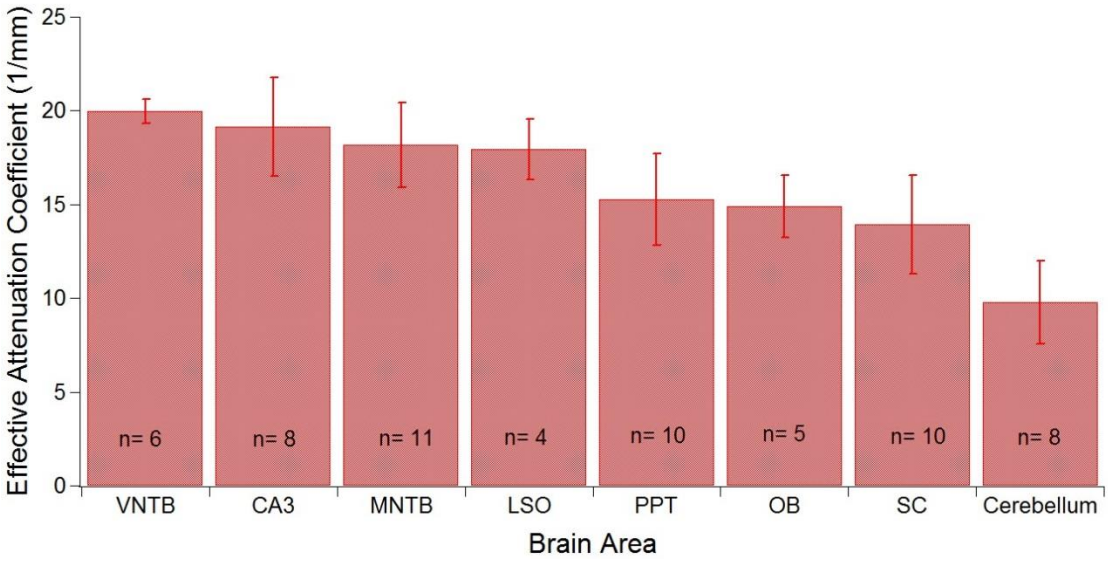

Figure III.8 Effective attenuation coefficients with SEMs for the eight brain areas: VNTB 19.96 +/- 0.26 (1/mm); CA3 19.12 +/- 0.84 (1/mm); MNTB 18.16 +/- 0.69 (1/mm); LSO 17.92 +/- 0.80 (1/mm); PPT 15.26 +/- 0.78 (1/mm); OB 14.88 +/- 0.74 (1/mm); SC 13.91 +/- 0.83 (1/mm); Cerebellum 9.76 +/- 0.78 (1/mm)

The MNTB, VNTB and LSO were measured with three wavelengths of light, while all other nuclei were measured with one wavelength, (see table III.1 for summary). One set of measurements was performed per brain nucleus per hemisphere.

Table III.1 Brain areas that were measured with three different wavelengths, and sample size (the unit of the effective attenuation coefficient is 1/mm) [12]

Brain Area	Effective Attenuation Coefficient μ_{eff} (1/mm)		
	λ1= 453 (nm)	λ2= 528 (nm)	λ3= 940 (nm)
MNTB	18.16 (n=11)	15.86 (n=9)	13.86 (n=8)
VNTB	19.96 (n=6)	17.69 (n=7)	14.39 (n=7)
LSO	17.92 (n=4)	15.91 (n=7)	14.01 (n=6)
PPT	15.26 (n=10)		
SC	13.91 (n=10)		
CA3	19.12 (n=8)		
Cerebellum	9.76 (n=8)		
Olfactory	14.88 (n=5)		

Figures III.9 and figure III.10 show the practical consequences of these differential coefficients on light penetration through the different types of tissue. Figure III.9 plots the optical power required to illuminate neurons up to a tissue depth of 300 μm below the optical fiber tip with a light intensity of at least 10 mW/mm^2 (the light power required for ChR2 activation 8-12mW/mm^2 [3]). To achieve this goal in cerebellar cortex, about 1.5 mW need to be emitted from the tip of the optical fiber, while in the case of VNTB, about 20 times as much optical power is required to achieve the same goal.

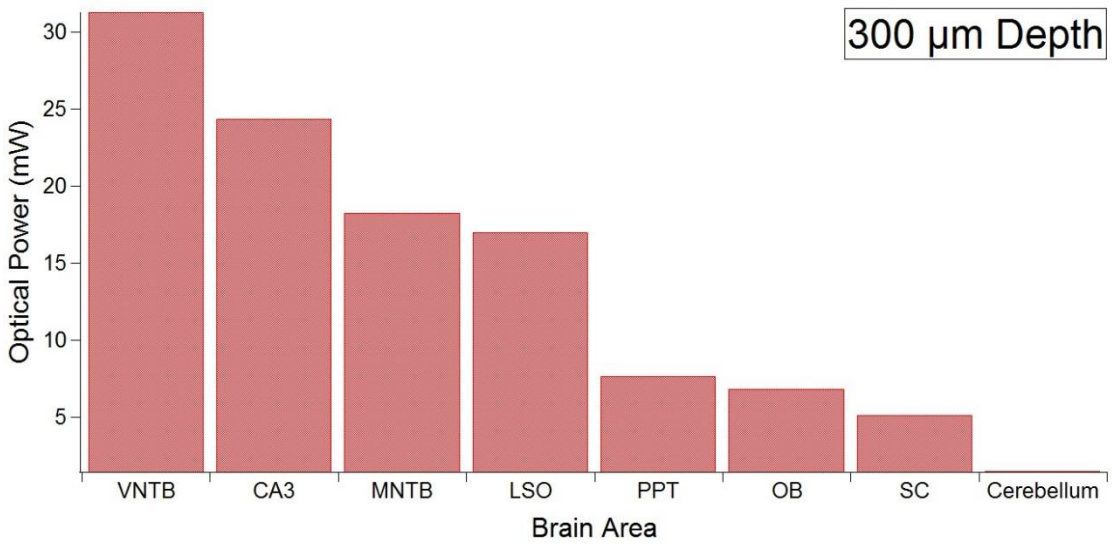

Figure III.9 Optical power values that would need to be fed into a 100 µm diameter optical fiber when 300 µm of tissue needs to be illuminated at intensities typically used for Channelrhodopsin activation

Due to the nonlinear nature of light distribution in tissue, these differences become more dramatic for deeper penetration. For example, doubling the illumination depth from 300 µm to 600 µm would require about 20x the light intensity in the case of cerebellar cortex tissue (28 mW). By contrast, illuminating 600 µm of VNTB tissue to the same degree would require 12 W of light intensity, or 400 times the intensity required to illuminate 300 µm (Figure III.10).

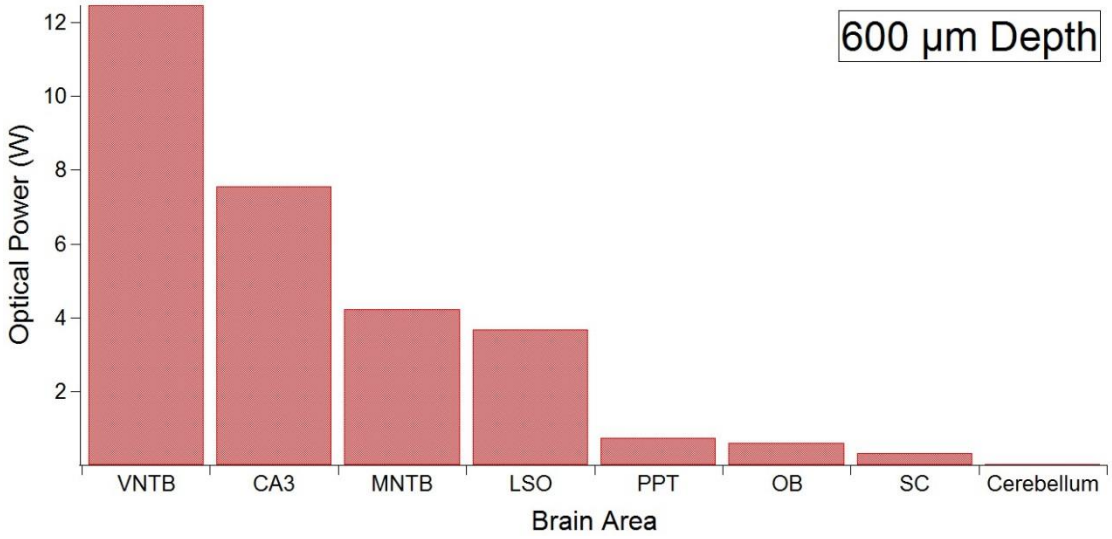

Figure III.10 Same as figure III.11 except that in this example the illumination was calculated to hypothetically activate Channelrhodopsin over a distance of 600 µm from the fiber tip

These calculations suggest substantial differences in light scattering among different brain areas, and make the point that certain manipulations are possible in some brain areas but not others.

Light Scattering Varies with Wavelength

A traveling wave interferes with objects that are larger than its wavelength, but tends to bend around objects smaller than its wavelength. Thus, long wavelength light penetrates tissue deeper than short wavelength light. Since different lightsensitive molecules are optimally excited at a variety of wavelengths, we tested the influence of light wavelength on the penetration depth of light in brain tissue. Figure III.11 represents experiments in which MNTB was tested with three wavelengths: 453 nm, 528 nm, and 940 nm. As expected, the longest wavelength (940 nm) showed the most effective penetration, i.e. the smallest attenuation of light intensity with increasing distance from

the fiber tip (red line), while the blue light (453 nm) attenuated within the shortest distance from the fiber tip (blue line).

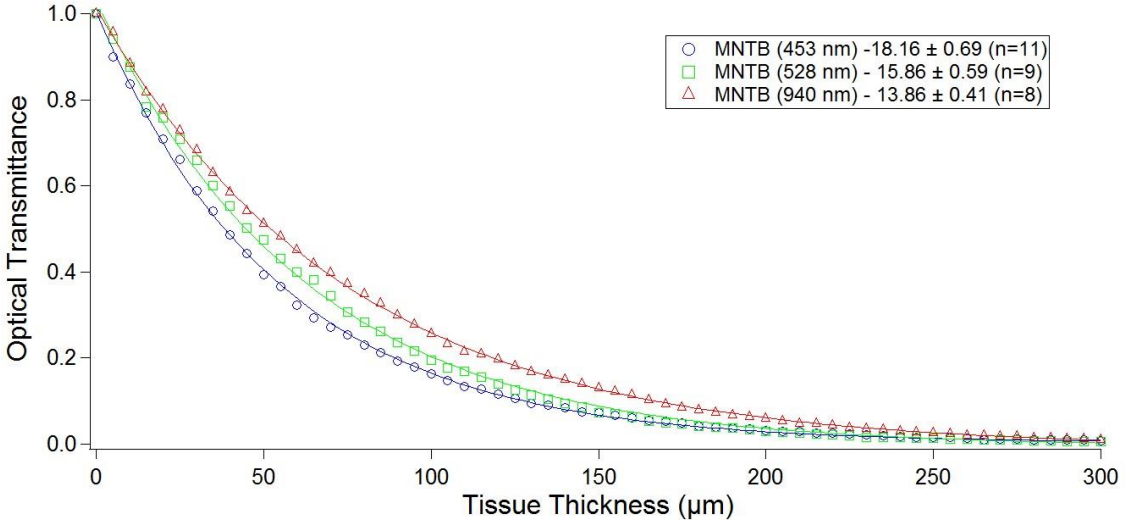

Figure III.11Effects of wavelength on optical transmittance. Optical transmittance in the MNTB as a function of tissue thickness and optical wavelengths. The three colorcoded data sets represent corresponding measurements with light of three different optical wavelengths (blue (453 nm), green (528 nm), and red (940 nm)). Longer-wavelength light penetrates tissue deeper, resulting in a higher transmittance at any given tissue thickness [12]

Similar observations were made for a second brain area (VNTB) that was tested in the same way (Figure III.12).

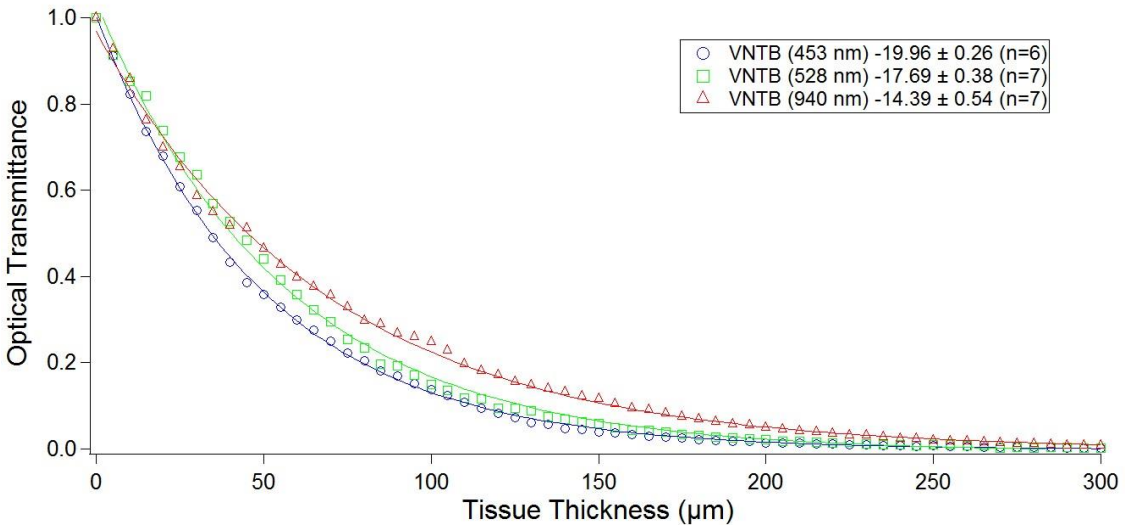

Figure III.12 Optical transmittance in the VNTB as a function of tissue thickness and optical wavelengths. The three colorcoded data sets represent corresponding measurements with light of three different optical wavelengths (blue (453 nm), green (528 nm), and red (940 nm)). Longer-wavelength light penetrates tissue deeper, resulting in a higher transmittance at any given tissue thickness

Note that optical absorption cannot be neglected at all light frequencies (an assumption made for the three single light frequencies tested in this study), and thus there is no simple linear extrapolation between the points shown in figure III.13 [18].

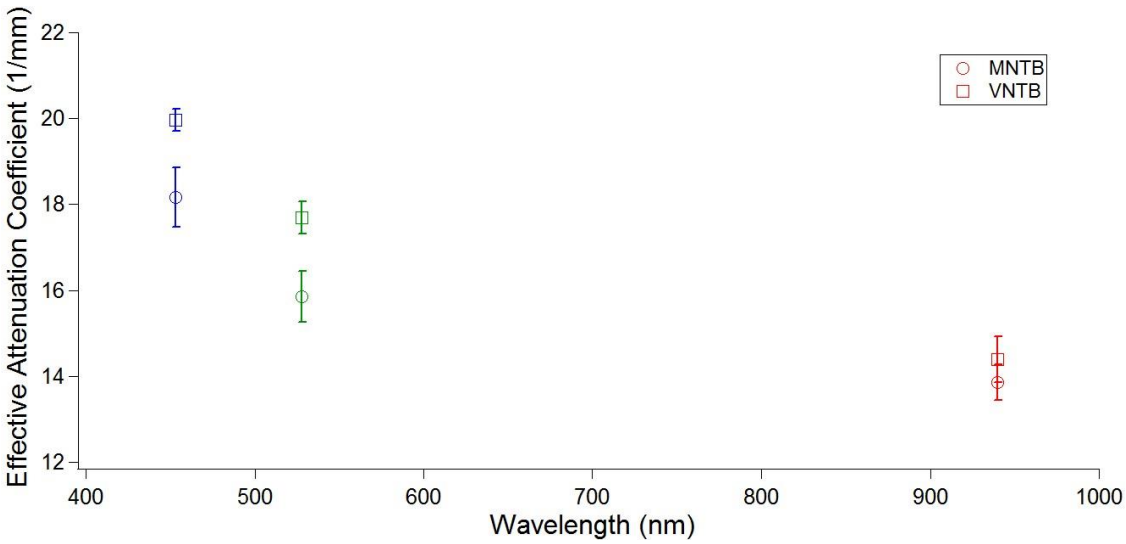

Figure III.13 Effects of light wavelength on transmittance in two brain areas (MNTB and VNTB). The effective attenuation coefficient decreases with wavelength for the three wavelengths tested. MNTB measurements are represented by round symbols while VNTB measurements are represented by square symbols. Measurements in the three different colors are indicated by the color-code of the symbols [12]

While the datapoints can be fitted with a single exponential (Figure III.14), the relationship may be more complex [18].

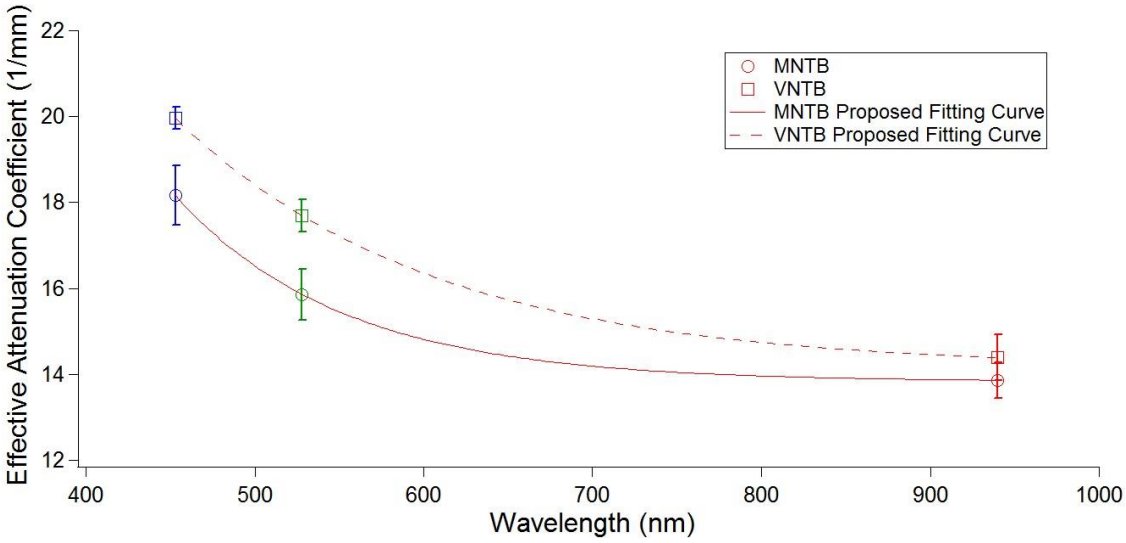

Figure III.14 MNTB and VNTB proposed fitting curves for the effective attenuation coefficients as a function of wavelengths

Light Scattering Brain Atlas

While the fiber punch-through method allowed for measurements of light scattering properties in anatomically defined brain areas, it is a relatively slow method. Measuring many different brain areas with this technique would not be feasible. However, to extend usage of our data to other areas of the brain without the need for additional punch-through measurements, we prepared a brain atlas containing light scattering values from the entire mouse brain. For this atlas, sections of 300 μm thickness were prepared from mouse brains, and imaged with an Olympus virtual microscopy system (Olympus VS 120) using monochromatic transmitted light (546 nm band pass filtered with a 20 nm band-pass width). The resulting images consist of relative differences in tissue translucency in grey scale between different brain areas in the section. Figure III.15 shows an example of such an image, with several nuclei marked with colored lines on the section.

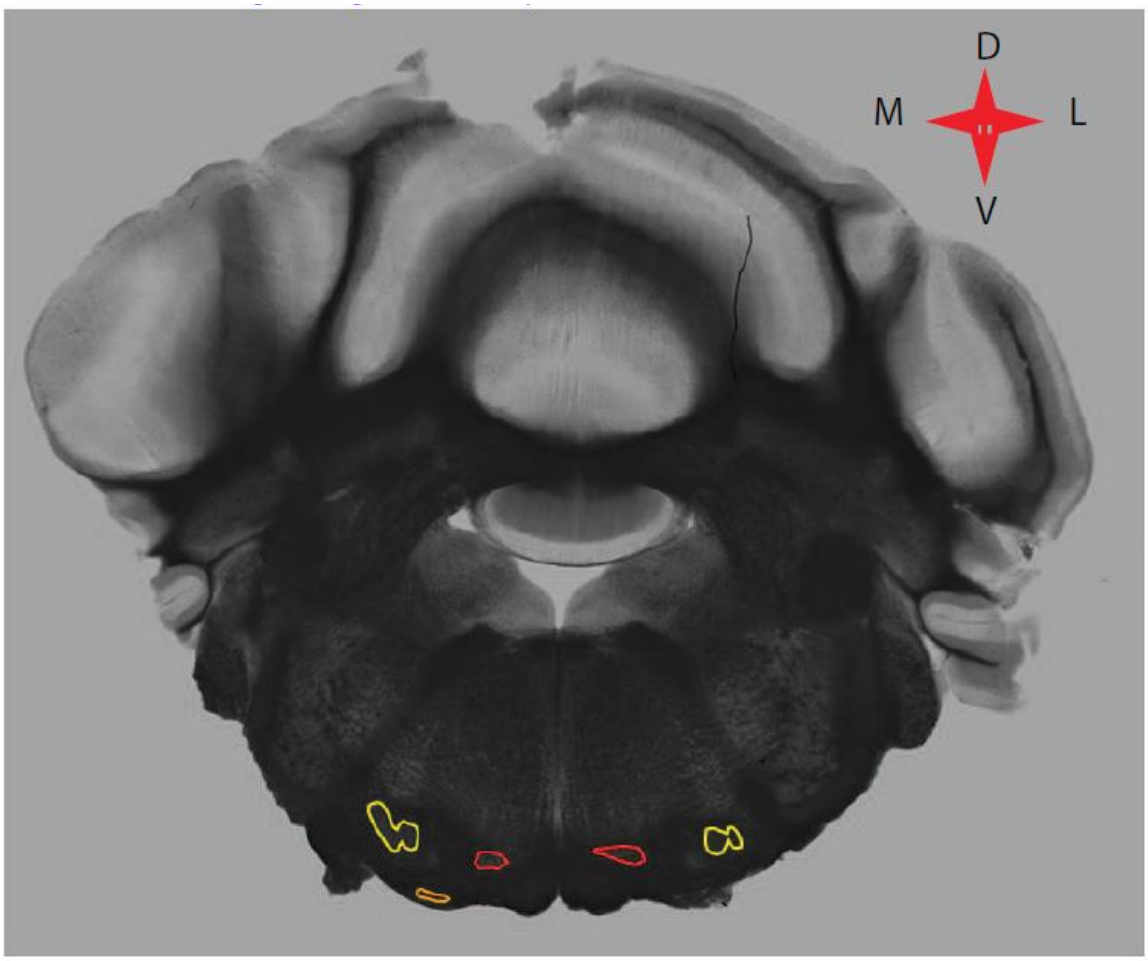

Figure III.15 Relating fiber punch-though measurements to brain atlas measurements. An image of a 300 µm coronal section of mouse brain stem, taken on a calibrated virtual microscopy system with monochromatic light. Areas with higher optical transmittance appear brighter on the image, while areas with lower transmittance appear darker. MNTB, VNTB, and LSO are outlined in red, orange, and yellow, respectively [12]

For brain areas that were also measured with the punch-though method, the relative grey values of the images correlated very well with the effective attenuation coefficients measured with the punch-through method (Figure III.16), suggesting that the grey values of the images can be used as a basis to calculate the effective attenuation coefficients for brain areas that have not been tested with the punchthrough method.

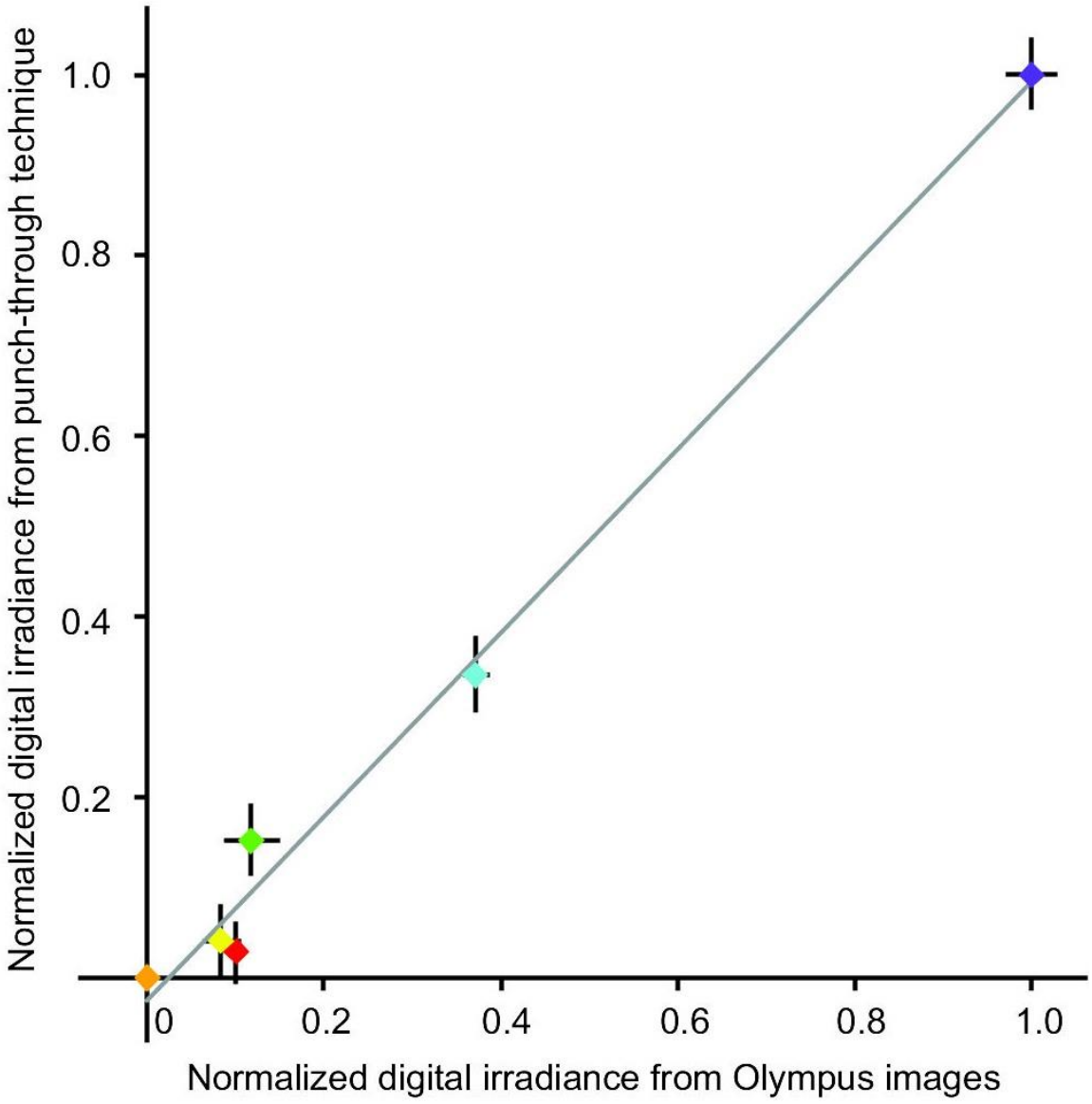

Figure III.16 Correlation in digital irradiance for brain areas tested with both the fiber punch-through and the virtual microscopy method. Digital irradiance was measured in six brain areas (MNTB (red), VNTB (orange), LSO (yellow), PPT (green), SC (light blue), and cerebellum (dark blue) with both the fiber punch through and the virtual microscopy technique. Results were normalized and plotted against each other. Each colored symbols represents the measurements from one brain area with two methods, the solid line indicates complete overlap between the measurements. The bars attached to each data point represent the standard error [12]

Importantly, the grey value images in combination with the effective attenuation coefficients measured with the punch-through method allowed us to establish an atlas of brain translucency that can be used to calculate the light scattering properties of any brain area in the adult mouse brain.

Applying the Data to Experimental Design

An investigator planning an experiment involving light activation of a given protein *in-vivo* is typically interested in the amount of light required to activate the protein at a distance d, from the fiber tip. In order to correctly determine the required amount of light, the following parameters must be considered: 1) The wavelength of the light, 2) the largest distance from the fiber tip at which proteins are to be activated, 3) the specific light scattering properties of the brain area involved, and 4) the diameter of the fiber tip. We produced a computer program that calculates the required amount of light for a given experiment based on user input of these parameters. Screenshots from this computer program can be seen in the following figures. The program also incorporates the brain atlas described above. For further information, see www.optogeneticsapp.com.

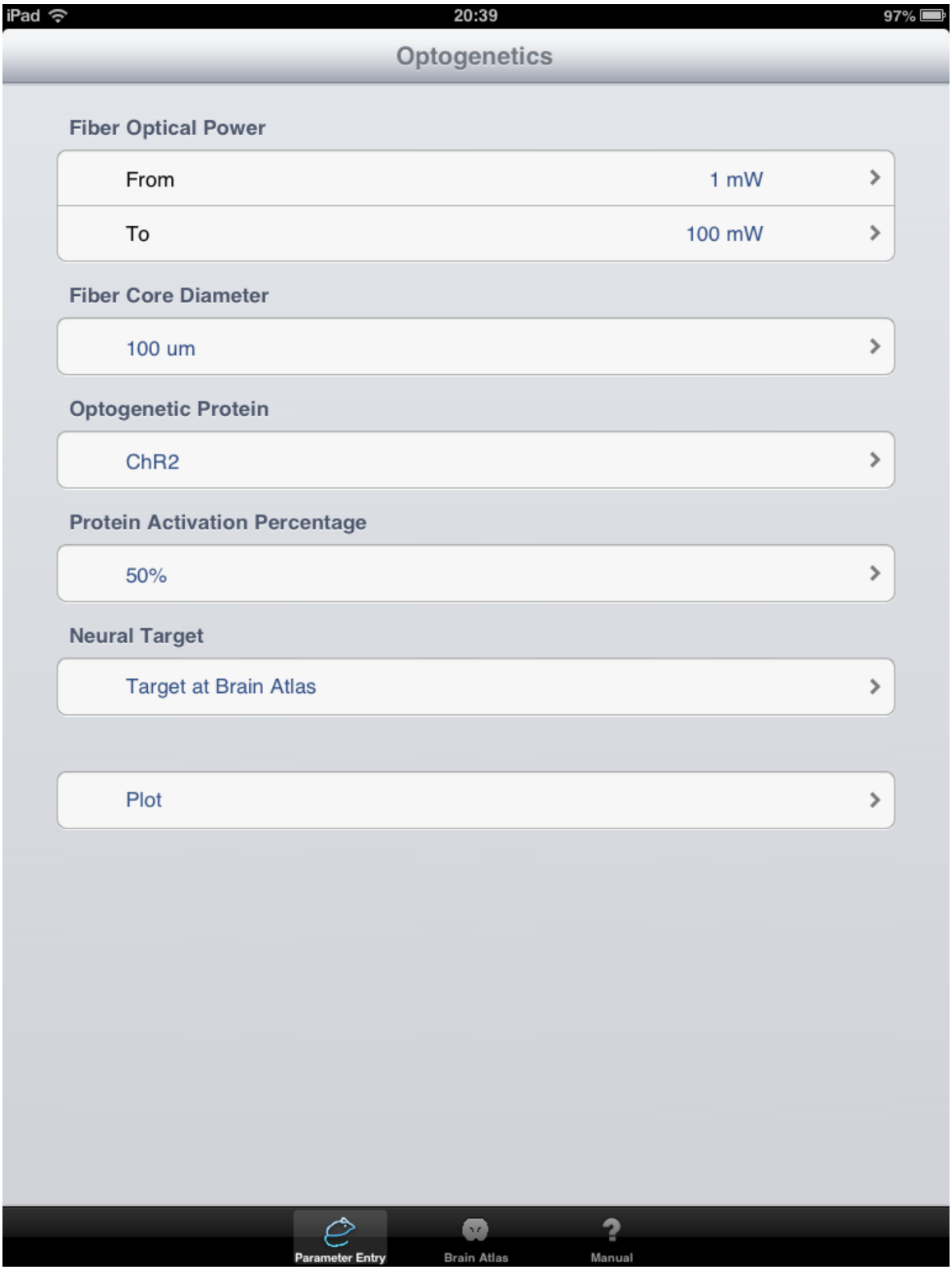

Figure III.19 The desired input parameters control panel

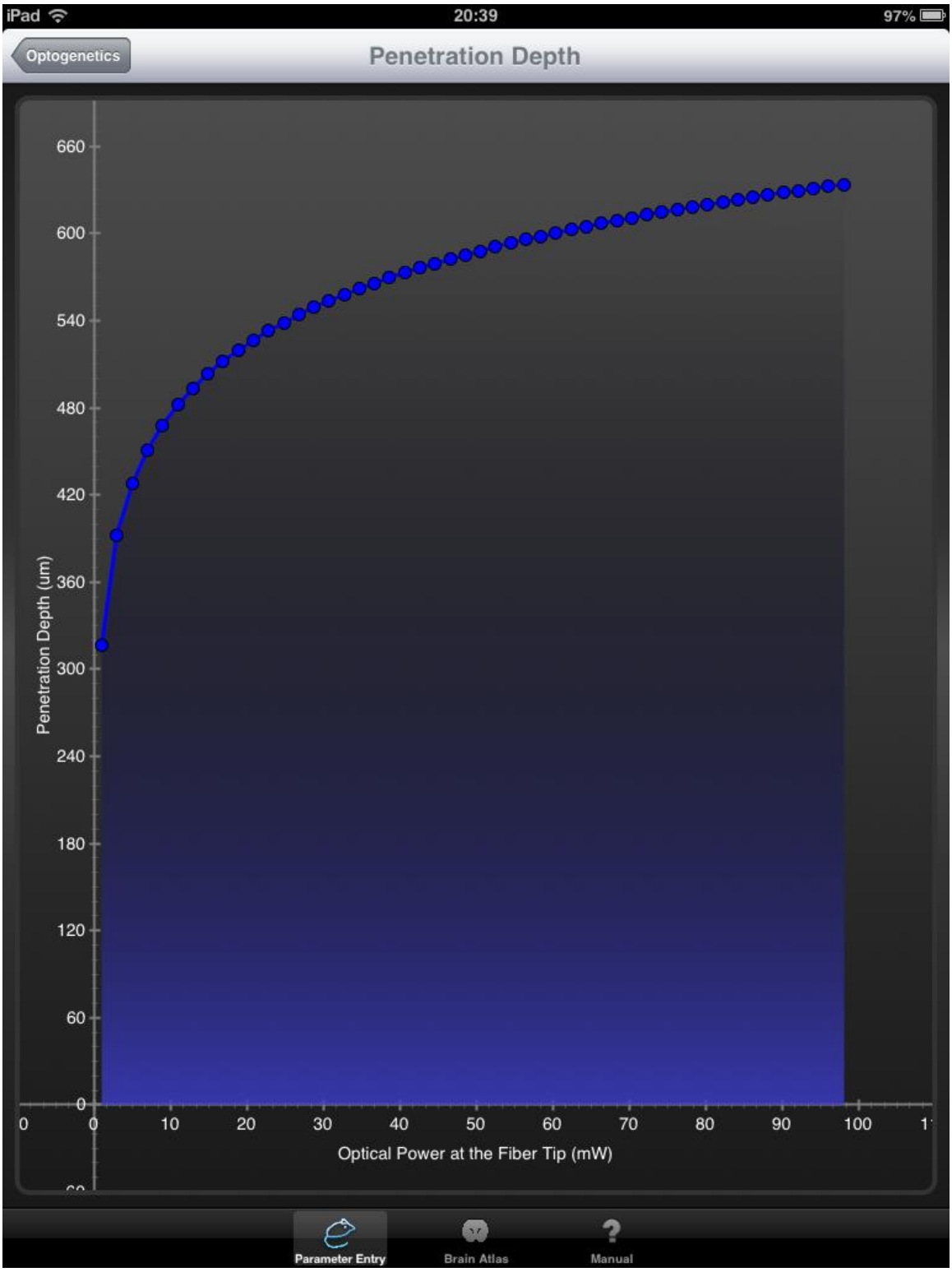

Figure III.20 The attainable penetration depth as a function of optical power at the fiber tip for the desired entered input parameters

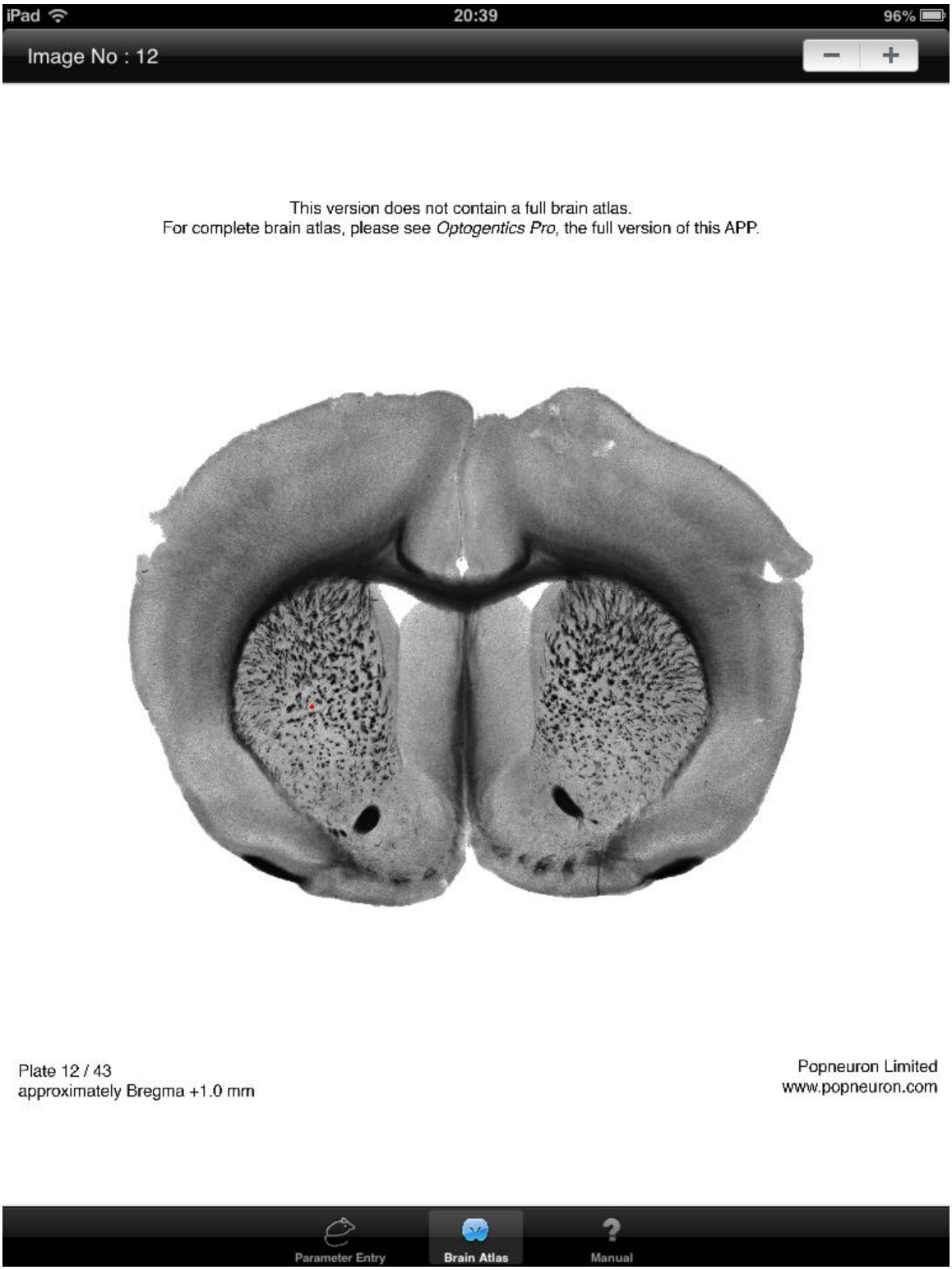

Figure III.21 A sample image from the brain atlas where the investigator can select the area of interest precisely such that its optical properties are designated, and the corresponding penetration depth and optical power at the fiber tip are calculated, accordingly

iPad 20:40 96%

Optogenetics
Version 2.2
User Manual

Overview:

Optogenetics is a tool that aids an investigator in calculating the required optical power for a given *in-vivo* experiment involving optogenetics or any other experimental approach that includes light delivery to deep brain areas via optical fibers. To estimate the amount of light required for a given experimental design, knowledge about the specific scattering properties of the brain region of choice, the specific opsin to be used, and the properties of the optical fiber are required. A user enters these parameters into the APP, which then calculates the light scattering for the specific experimental situation. The APP includes a full brain atlas for the adult mouse brain (Pro Version), from which a user can look up the specific scattering properties of the brain area of choice. All data and all computations that are used in this APP are published in: Al-Juboori, Dondzillo, Stubblefield, Felsen, Lei, and Klug: Light scattering properties vary across different regions of the adult mouse brain. PlosONE, in press.
For more information, pls see www.optogeneticsapp.com.

Parameter Entry Screen:

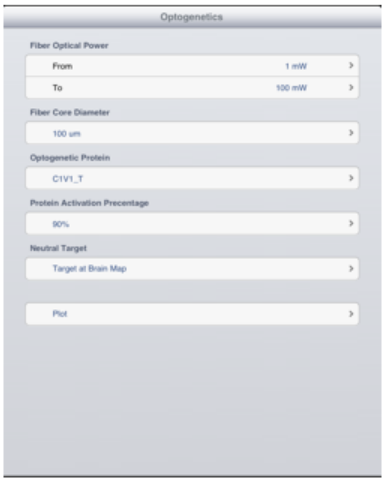

The *Parameter Entry* screen has six data entry fields into which the desired experimental parameters can be entered, either via drop-down menus, or via the keyboard.

The six parameters are:

Fiber Optical Power:
Enter the minimum and maximum optical power you wish to use, or that your equipment is able to produce. The penetration depth plot (see below) will plot the maximum penetration depth for each power value between the minimum and maximum power values set here.

Fiber core diameter:

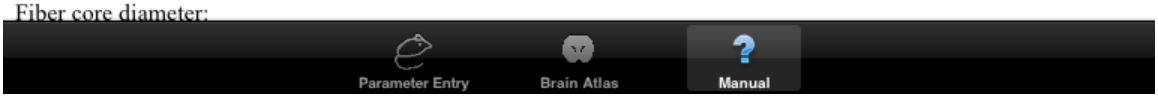

Figure III.22 A screenshot for the user manual that is available in the computer program also, in which the user can be taken through details about how to use this application to its full extent

CHAPTER IV

DISCUSSION AND MAIN FINDINGS

Discussion

This study has been dealing with a lot of cardinal questions about the best approach that these measurements must be conducted in order to make its main tasks achievable. It has also been tackling many technical and practical issues; however, these problems have eventually been overcome by modifications for the system setup.

So far this study has shown that it could be a necessity to choose different illumination profiles and sources to activate some brain areas maybe through various light profiles or side emitting fibers…etc. It has also been acknowledged that the regions under study can be arranged from the densest to the least optically dense as VNTB, CA3, MNTB, LSO, PPT, OB, SC,and Cerebellum, respectively, as illustrated in figure III.8.

Another crucial aspect that this study has explored is the optical properties age dependence for those brain tissues within the same species. Moreover, it has also shown how important the tissue health is and how it affects the measurements all in all, and how the time degradation rate for those brain tissues play a major role in their optical characteristics. Most importantly, it shed light on the situation when there is a photosensitive florescent material within the same region that is highly likely to emit light back after being shining with a certain wavelength which gives awkwardly incorrect results. And definitely this phenomenon should be avoided or resolved somehow.

On the flip side, there are still few "on stage" complexities that should be mitigated. One of which is the camera saturation when it comes to very thin sample

thickness and that decreases the number of points that are taken for curves construction and narrow the total moving distance, and eventually, it becomes obscure for the fitting program to establish the best fitting approach. Another problem that has happened sometimes is what so-called, humorously, "the pillow effect". Simply, it's the same response that a pillow might respond when it is pushed from the middle and that will be lifting its sides up higher. Applying this on a sample with one of the threads or strings in the middle will lead to the same results and might alter the readings severely, sometimes.

Yet, altogether, this study is still promising, especially, for the methodology of doing it this way that has not been done widely.

Main Findings

There are four main findings of this study: 1) Light emitted into brain tissue from a point source such as an optical fiber declines exponentially in intensity with increasing distance from the fiber tip 2) There are substantial differences in light scattering properties among different brain neural areas, resulting in a need for specific knowledge about any given brain area to be illuminated 3) The light wavelength used in a particular experiment additionally influences the scattering properties, with longer wavelength light penetrating deeper into the tissue 4) The results obtained in this study could be integrated into a brain atlas of light scattering in the mouse brain, as well as a computer program that allows a user to easily determine the light requirements for any given experimental situation.

The most important finding is the observation that there are substantial differences in the optical properties across different brain areas. For simplicity, previous studies have assumed that light propagation through brain tissue is similar throughout the

brain, and have calculated the light requirements for optogenetic experiments with a single effective attenuation coefficient [1], [10], [11]. Our results show that a differential approach is needed, because the observed differences in effective attenuation coefficients can have substantial consequences on experimental design. Figure III.9 and figure III.10 illustrates this point and suggest that certain manipulations are possible in some brain areas but not others.

In some experiments, one might want to restrict the volume of illumination, e.g. if an opsin is widely expressed in the brain [19] but only a certain region is to be manipulated with light. Thus, specific knowledge of the light requirements for a given experimental situation can inform an optimal experimental design, and this includes knowledge about the specific light attenuation properties of the brain area to be manipulated, as well as knowledge about how different light wavelengths will affect the illumination.

CHAPTER V

IMPROVEMENTS, COMPARISON WITH PREVIOUS STUDIES, AND FUTURE PLANS

Improvements

A handful of improvements that would shift the accuracy and performance to the edge are being thought seriously to be incorporated at this stage of doing this research toward perfecting a three-dimensional (3D) light attenuation model for the brain. One of these enhancements is to find out a more positive way to tell whether the fiber tip is right at the top of sample surface neither far away from it, nor punched through it. Another interesting scheme to measure would be obtainable by inserting some mechanical properties that the sample could be described with to resolve the mystery behind the actual act that is happening while the optical fiber is punching through, for instance; is it punching through smoothly, pushing it to other sides through a random process, or tearing the sample (which might be one of the reasons why there has been CCD camera intensity saturations happening at some points when the fiber tip gets closer to the bottom of the chamber). Hopefully, that will lead to an optomechanical three-dimensional (3D) model for the light being attenuated in those brain areas.

Another empirical idea that has been come up with, recently, is what it could be established by some minor adjustments to the system setup by changing the optical intensities for the optical fibers that will be traversing a specific sample thickness through tuning the current intensity. That allows erecting, at least, two handy graphs for each sample thickness associated with a certain optical fiber manufacturer specifications and

the wavelength used. One of them would be the actual initial optical power intensity measured at the sample surface as a function of current intensity- for a specific laboratory experimental setup. The other one is the optical power intensity measured after the light makes it through the whole sample thickness as a function of the initial one that has been started with. Having done that, it will provide actual real numerical values for the optical intensities needed to be delivered to carry out the desired action with the corresponding initial ones that they should be started with in hand for the targeted brain area embedded under certain depth. The results of this experiment could be incorporated with and used for further examination, solidification, and confirmation to the results of this study.

Comparison with Previous Studies

Aravanis and colleagues [1] first characterized the optical scattering effect in mouse brain cortical tissue by measuring the optical attenuation at different slice thicknesses. In their work, the Kubelka-Munk model ($T = 1/(S \cdot z + 1)$ where S is the scattering coefficient) was used in their data fitting. However, our measurements were best fitted with an exponential function and the data cannot be satisfactory fitted with the Kubelka-Munk equation. The discrepancy mainly occurs at larger distances ($z > 200\ \mu m$), and our data show that light attenuates much faster than predicted by the Kubelka-Munk model, resulting in a much reduced excitation distance of neural targets in our results. A comparison between the two different fitting equations on a PPT raw data is shown in figure V.1.

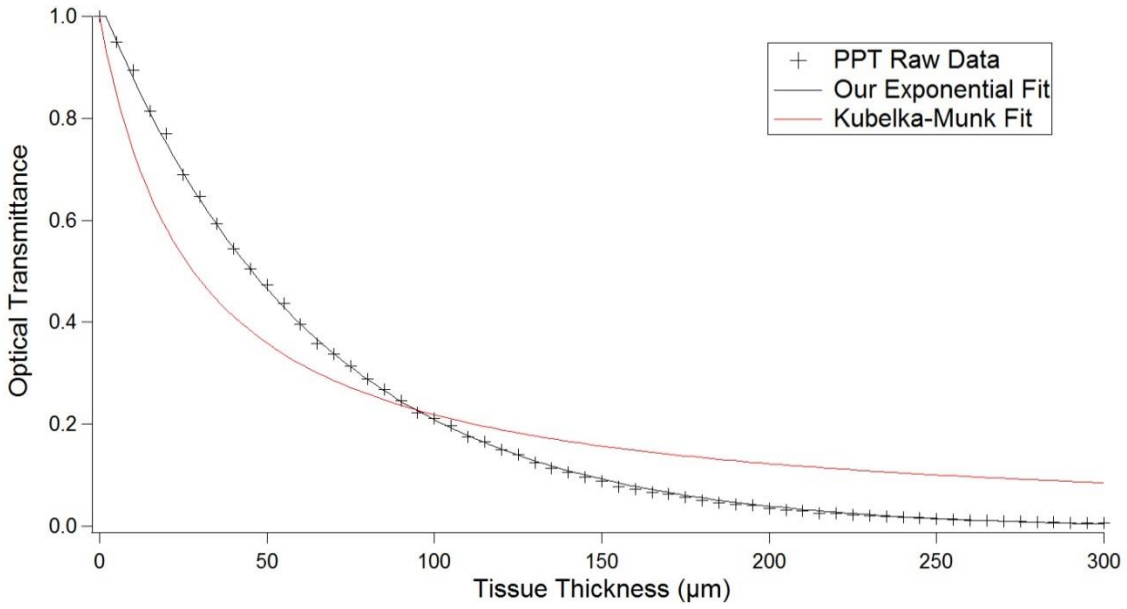

Figure V.1 A comparison between our exponential fit and Kubelka-Munk fit for a PPT raw data showing that it is best fitted with a single exponential curve

More recently, Stark et al. [20] report that their measurements of optical attenuation at larger distances from the fiber tip cannot be well fitted with the Kubelka-Munk equation, although at shorter distances the data fit with the equation is good. The differences are likely due to the different optical detectors being used in these experiments. In our measurements, a single pixel of the CCD camera along the center of the propagation axis of the optical fiber was used to construct the optical transmittance curve. By contrast, the previous studies used a large area photodetector to measure the optical attenuation, which also collects light not strictly propagating along the optical axis. This difference could potentially result in differences in the data. Having taken that into account, total intensity measurements were calculated and averaged over the entire detector's area, and the results still indicate that the data can not be well fitted with the Kubelka-Munk equation but rather a single exponential curve as shown in figure V.2.

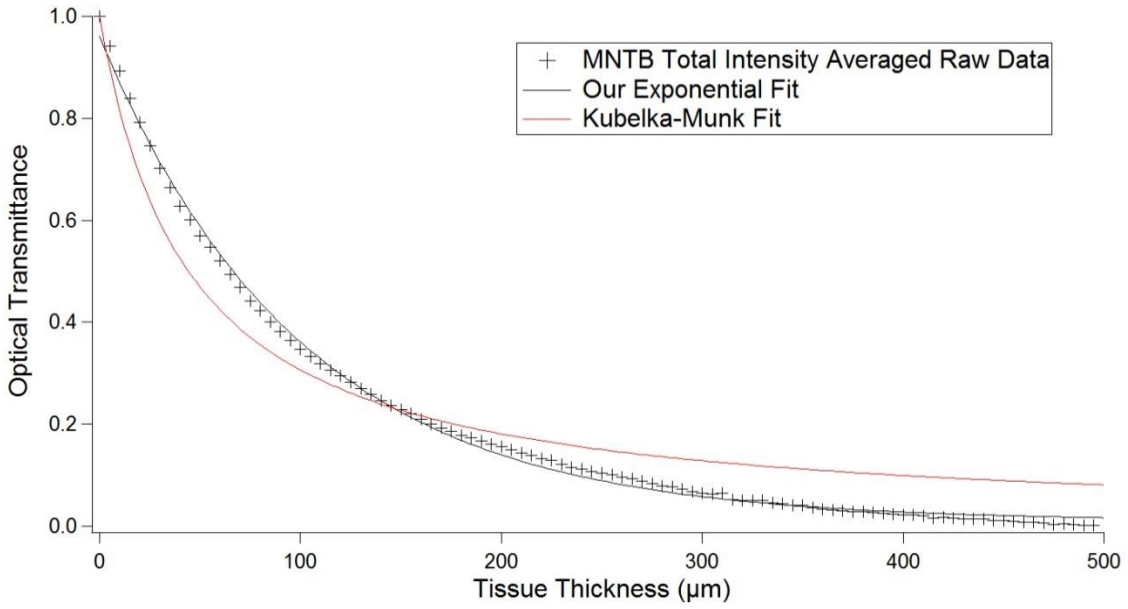

Figure V.2 A comparison between our exponential fit and Kubelka-Munk fit for an MNTB total intensity measurements of the raw data averaged over the entire detector's area showing that it is best fitted with a single exponential curve

When light comes out of an optical fiber tip, light spread as well as the radius of light increases as light propagates further away from the fiber output. This cone shape of light propagation increases the beam area (A), thus reducing the optical irradiance of the light beam $(I = P/A)$. However, this reduction of optical irradiance due to beam spreading from the optical fiber is much more gradual than the optical scattering in the brain tissue, so this beam spreading effect can be neglected or considered to be absorbed in the effective attenuation coefficient μ_{eff}. For example, the numerical aperture (NA) of the $100\ \mu m$ core $(r = 50\ \mu m)$ diameter optical fiber that was used in 0ur measurement is 0.22, such that the acceptance angle θ of the light cone is 9.5 degree $(NA = n \sin^{-1}\theta\ \ where\ n = 1.33\ in\ water)$. The radius of the beam increases over a propagation distance of $d = 500\ \mu m\ by\ 83\ \mu m$ $(\delta r = d \tan\theta)$; thus the beam area increases by a factor of 7, resulting in an optical irradiance reduction to 14% of its

original output. At the same time, according to our measurements, the optical transmittance of the MNTB due to optical scattering after $500\ \mu m$ of propagation is 0.01% at 453nm wavelength. Therefore, we conclude that the optical fiber beam spreading is not a significant effect in estimating the optical irradiance in brain tissues.

Future Plans

Application of the Findings to Future Experiments

One goal of this study was to provide a body of knowledge on light scattering properties of the mouse brain that could be used by investigators as a tool to optimize the light stimulation for a specific experimental situation. To this end, data from several brain areas were collected but the fiber punch-through method, while allowing us to obtain data in great detail, was not efficient enough to use for a multitude of brain areas. Therefore we resorted to virtual microscopy to image the entire mouse brain with monochromatic transmitted light. The resulting images consisted of gray-value pixels, which represented the differences in optical properties between these different brain areas. The differences in grey values between different brain areas obtained with virtual microscopy corresponded well with the differences observed in the fiber punch-through method, allowing us to calibrate the results from the two approaches to each other. Thus, we obtained data on the light scattering properties of the entire mouse brain, allowing an investigator to look up the brain area of choice in the light scattering atlas, and determining the associated specific effective attenuation coefficient for that area. This coefficient can be entered into a computer program, together with information on the desired stimulation wavelength and volume of brain tissue to be illuminated super-

threshold. The computer program then estimates the required light intensity at the optical fiber tip to meet the desired criteria. The use of these tools should allow an experimenter to design optogenetic manipulation *in-vivo* with better precision and more confidence that the brain area to be activated by light will actually be illuminated at a super-threshold intensity. Moreover, the delivered light can be adjusted to be super-threshold for opsin activation in the desired brain area, and fall to sub-threshold values at the borders of the brain area of interest, reducing unspecific activation of adjacent neuronal areas. For further information, see www.optogeneticsapp.com.

Research Proposal for Determining Diffusivity Constants for Individual Brain Areas

While the concept of using Optogenetics is growing tremendously and becoming more involved in a variety of research and development studies in the field of neuroscience and some other relevant branches which could be: robotics and neural networks and fuzzy control soft computing (maybe in the future), there are still a handful of related parameters to this methodology that require more investigation and some of which are still undetermined. For example, the optical, mechanical, and thermal properties of different brain areas. The knowledge about those parameters is of significant importance to achieve the desired activation or stimulation for those targeted brain areas precisely, accurately, and without damaging the brain tissues. In this experiment we are interested in determining the conductivity or diffusivity constants for individual brain areas. This will introduce the idea of delivering above the threshold amount of optical power intensity assumed to activate the neurons from cortex, without having the optical fiber punch through them; using a pulsed laser with specific

parameters. For instant, the pulse energy, the pulse duration or the pulse width, and the Pulse Repetition Rate (PRR)- that match those conductivity or diffusivity constants under study. Having done that, the heat accumulation and the consequent brain tissue damage that is expected to happen via using Continuous Wave (CW) lasers of high-power will be compensated for. If the threshold optical power intensity for a targeted area, the effective attenuation coefficient due to scattering and absorption phenomena per unit length, and the conductivity or diffusivity constant (unit power per unit length per unit time; i.e. $(mW\ mm^{-1}s^{-1})$ were known, and after a few calculations, all it is needed to do is to match the time required for that pulse to reach a certain depth with PRR for the laser. In that case, the energy will be transferred to the targeted spot, and at the same time, get rid of the excessive energy that will be building up if the laser source was functioning in a CW mode; through the diffusing process of that energy during the off-mode between pulses. In order to carry out this experiment, a sample from the area under investigation will be labeled by two different types of fluorophores: Midori-Ishi Cyan (MiCy)- one of the Cyan Fluorescent Proteins (CFP)s, and mRFP1- one of the Red Fluorescent Proteins (RFP)s. Those two Fluorophores have the properties shown in table V.1.

Table V.1 Midori-Ishi Cyan and mRFP1 properties [21]

Fluorophore Type	Excitation Maximum (nm)	Emission Maximum (nm)	Molar Extinction Coefficient	Quantum Yield	In vivo Structure	Relative Brightness (% of EGFP)
Midori-Ishi Cyan (MiCy)	472	495	27,300	0.90	Dimer	73
mRFP1	584	607	50,000	0.25	Monomer	37

In addition to that, their excitation and emission spectra are illustrated in figure V.3 and figure V.4.

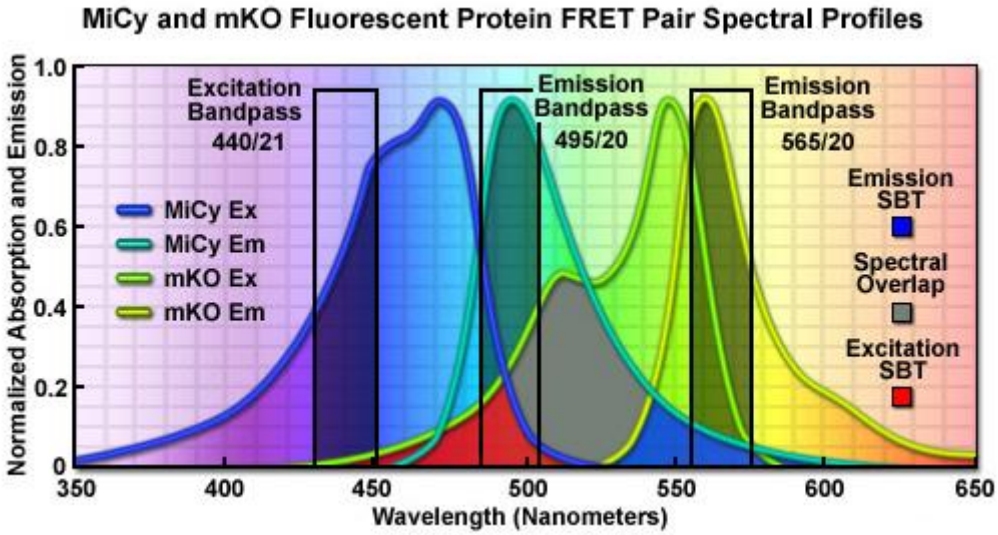

Figure V.3 MiCy excitation and emission spectra [22]

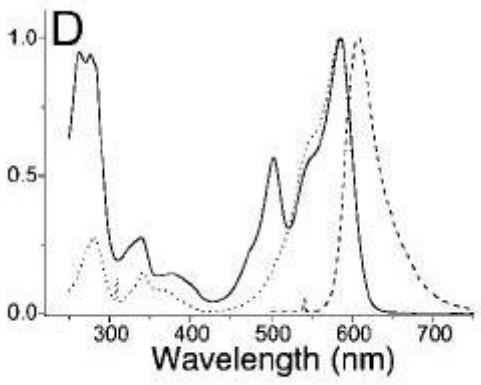

Figure V.4 mRFP1 absorption (solid line), excitation (dotted line), and emission (dashed line) spectra [23]

Those probes are suitable for conducting this experiment for their excitation peaks pretty close to the activation maxima for Channelrhodopsin-2 (ChR2) which is approximately 470 nm and Halorhodopsin (NpHR) which is approximately 580 nm [9]; where ChR2 and NpHR are the fundamental constituents of any Optogenetics study. Their activation spectra are depicted in figure V.5.

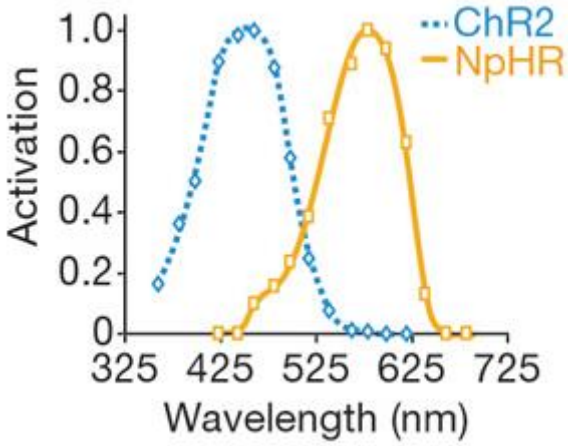

Figure V.5 ChR2 and NpHR activation spectra [4]

From light sources perspectives, this experiment can be operated with one of the EPL series of Picosecond (ps) Pulsed Diode Lasers; like the ones from Edinburgh Instruments with a wavelength of 470 nm and featuring 10 set repetition frequencies from 20 kHz to 20 MHz and pulse widths down to ca. 70 ps [24]. Whereas, the 580 nm wavelength could be obtained from an Nd:YAG laser (1064 nm) after a frequency doubling process followed by Q-switching operation to get the desired pulse shape [25]. These light sources will be attached and coupled to optical fibers, and some of their specifications such as: energy, both duration or width, and PRR would be highly preferred to be adjustable and tunable. Moreover, some wavelength selection filters could be used, as well, to improve and optimize the system experimental set-up and performance.

REFERENCES

1. Aravanis AM, Wang LP, Zhang F, Meltzer LA, Mogri MZ, Schneider MB, Deisseroth K (2007) An optical neural interface: in vivo control of rodent motor cortex with integrated fiberoptic and optogenetic technology. *J Neural Eng* 4: S143-56.

2. Boyden ES (2011) A history of optogenetics: the development of tools for controlling brain circuits with light. F1000 Biol Rep 3: 11.

3. Boyden ES, Zhang F, Bamberg E, Nagel G, Deisseroth K (2005) Millisecondtimescale, genetically targeted optical control of neural activity. *Nat Neurosci* 8: 1263–1268.

4. Zhang F, Wang L-P, Brauner M, Liewald JF, Kay K, Watzke N, Wood PG, Bamberg E, Nagel G, Gottschalk A, Deisseroth K (2007) Multimodal fast optical interrogation of neural circuitry. *Nature* 446: 633–639.

5. Bernstein JG, Garrity PA, Boyden ES (2012) Optogenetics and thermogenetics: technologies for controlling the activity of targeted cells within intact neural circuits. *Curr Opin Neurobiol* 22: 61–71.

6. Nowak VA, Pereira EA, Green AL, Aziz TZ (2010) Optogenetics—shining light on neurosurgical conditions. *Br J Neurosurg* 24: 618-24.

7. Henderson JM, Federici T, Boulis N (2009) Optogenetic neuromodulation. *Neurosurgery* 64: 796-804.

8. Lagali PS, Balya D, Awatramani GB, Münch TA, Kim DS, Busskamp V, Cepko CL, Roska B (2008) Light-activated channels targeted to ON bipolar cells restore visual function in retinal degeneration. *Nat Neurosci* 11: 667–675.

9. Zhang F, Aravanis A, Adamantidis A, de Lecea L, Deisseroth K (2007) Circuit-breakers: optical technologies for probing neural signals and systems. *Nat Rev Neurosci* 8: 577–581.

10. Gradinaru V, Mogri M, Thompson K, Henderson J, Deisseroth K (2009) Optical Deconstruction of Parkinsonian Neural Circuitry. *Science* 324: 354-359.

11. Chow B, Han X, Dobry A, Qian X, Chuong A, Li M, Henninger M, Belfort G, Lin Y, Monahan P, Boyden E (2010) High-performance genetically targetable optical neural silencing by light-driven proton pumps. *Nature* 463: 98-102.

12. Al-Juboori SI, Dondzillo A, Stubblefield EA, Felsen G, Lei TC, et al. (2013) Light Scattering Properties Vary across Different Regions of the Adult Mouse Brain. PLoS ONE 8(7): e67626. doi:10.1371/journal.pone.0067626.

13. Wang LV, Wu HI (2007) Biomedical Optics: Principles and Imaging. Wiley-Interscience.

14. Cheong WF, Prahl SA, Welch AJ (1990) A review of the optical properties of biological tissues. *IEEE Journal of Quantum Electronics* 26: 2166-2185.

15. Wilson RH, Mycek MA (2011) Models of light propagation in human tissue applied to cancer diagnostics. *Technology in cancer research & treatment* 10: 121-134.

16. Boas D, Culver J, Stott J, Dunn A (2002) Three dimensional Monte Carlo code for photon migration through complex heterogeneous media including the adult human head. *Optics express* 10 :159-170.

17. Henyey LC, Greenstein JL (1941) Diffuse radiation in the galaxy. *Astrophysics Journal* 93: 70-83.

18. Sardar DK, Zapata BM, Howard CH (1993) Optical absorption of untreated and laser-irradiated tissues. *Lasers in Med. Science* 8: 205-209.

19. Arenkiel BR, Peca J, Davison IG, Feliciano C, Deisseroth K, Augustine GJ, Ehlers MD, Feng G (2007) In vivo light-induced activation of neural circuitry in transgenic mice expressing channelrhodopsin-2. *Neuron* 54: 205-18.

20. Stark E, Koos T, Buzsáki G (2012) Diode probes for spatiotemporal optical control of multiple neurons in freely moving animals. *J Neurophysiol* 108: 349-363.

21. Piston DW, Patterson GH, Lippincott-Schwartz J, Claxton NS, Davidson MW Introduction to Fluorescent Proteins. Nikon Microscopy Website.

22. Piston DW, Claxton NS, Olenych SG, Davidson MW Applications in Confocal Microscopy: The Fluorescent Protein Color Palette. Olympus Website.

23. Campbell RE, Tour O, Palmer AE, Steinbach PA, Baird GS, et al. (2002) A monomeric red fluorescent protein. Proc Natl Acad Sci U S A 99: 7877-7882.

24. group EIT EPL series of Picosecond (ps) Pulsed Diode Lasers from Edinburgh Instruments. Direct INDUSTRY website.

25. Pask HM, Piper JA (1998) Practical 580 nm source based on frequency doubling of an intracavity-Raman-shifted Nd:YAG laser. Optics Communications Volume 148: p. 285-288.